PLOS ONE

RESEARCH ARTICLE

Determining engineering properties of ultra-high-performance fiber-reinforced geopolymer concrete modified with different waste materials

Fadi Althoey[1,2], Osama Zaid[3]*, Saleh Alsulamy[4], Rebeca Martínez-García[5], Jesús de Prado Gil[5], Mohamed M. Arbili[6]

1 Department of Civil Engineering, College of Engineering, Najran University, Najran, Saudi Arabia, **2** Science and Engineering Research Center, Najran University, Najran, Saudi Arabia, **3** Department of Civil Engineering, Swedish College of Engineering and Technology, Wah Cantt, Punjab, Pakistan, **4** Department of Architecture and Planning, College of Engineering, King Khalid University, Abha, Saudi Arabia, **5** Department of Mining Technology, Topography, and Structures, University of León, León, Spain, **6** Department of Technical Civil Engineering, Erbil Technical Engineering College, Erbil Polytechnic University, Erbil, Iraq

* Osama.zaid@scetwah.edu.pk

Citation: Althoey F, Zaid O, Alsulamy S, Martínez-García R, de Prado Gil J, Arbili MM (2023) Determining engineering properties of ultra-high-performance fiber-reinforced geopolymer concrete modified with different waste materials. PLoS ONE 18(5): e0285692. https://doi.org/10.1371/journal.pone.0285692

Editor: Parthiban Kathirvel, SASTRA Deemed University, INDIA

Received: January 21, 2023

Accepted: April 28, 2023

Published: May 22, 2023

Data Availability Statement: All relevant data are within the paper and its Supporting Information files.

Funding: The authors are thankful to the Deanship of Scientific Research under the supervision of the Science and Engineering Research Center at Najran University for funding this work under the research centers funding program with Grant No. (NU/RCP/SERC/12/17). The authors also extend their appreciation to the Deanship of Scientific Research

Abstract

Reprocessing solid waste materials is a low-cost method of preserving the environment, conserving natural resources, and reducing raw material consumption. Developing ultra-high-performance concrete materials requires an immense quantity of natural raw materials. The current study seeks to tackle this issue by evaluating the effect of various discarded materials, waste glass (GW), marble waste (MW), and waste rubber powder (WRP) as a partial replacement of fine aggregates on the engineering properties of sustainable ultra-high-performance fiber-reinforced geopolymer concrete (UHPGPC). Ten different mixtures were developed as a partial substitute for fine aggregate, each containing 2% double-hooked end steel fibers, 5%, 10%, and 15% GW, MW, and WRP. The present study assessed the fresh, mechanical, and durability properties of UHPGPC. In addition, to evaluate concrete development at the microscopic level due to the addition of GW, MW, and WRP. Spectra of X-ray diffraction (XRD), thermogravimetric analysis (TGA), and mercury intrusion (MIP) tests were conducted. The test results were compared to current trends and procedures identified in the literature. According to the study, adding 15% marble waste and 15% waste rubber powder reduced ultra-high-performance geopolymer concrete's strength, durability, and microstructure properties. Even so, adding glass waste improved the properties, as the sample with 15% GW had the highest compressive strength of 179 MPa after 90 days. Furthermore, incorporating glass waste into the UHPGPC resulted in a good reaction between the geopolymerization gel and the waste glass particles, enhancing strength properties and a packed microstructure. The inclusion of glass waste in the mix resulted in the control of crystal-shaped humps of quartz and calcite, according to XRD spectra. During the TGA analysis, the UHPGPC with 15% glass waste had the minimum weight loss (5.64%) compared to other modified samples.

at King Khalid University for funding this work through Small Groups Project under Grant No. RGP.1/116/43.

Competing interests: The authors have declared that no competing interests exist.

1. Introduction

Because of the fast growth in the world's population and the developing infrastructure at a more rapid pace in developing countries [1], Ordinary Portland cement (OPC) is a highly utilized material in the construction sector now [2]. From the construction sector, related to the sustainability point of view, the manufacturing of OPC partakes 25% to 35% in the outflow of carbon dioxide [3]. The OPC's production process releases a significant amount of carbon dioxide into the environment, which is harmful to the atmosphere [4, 5]. As a result, a massive proportion of research has been performed to produce substitute binder, which has a less negative impact on the atmosphere and is also eco-efficient [6, 7]. Consequently, the production of geopolymers material as a possible substitute for OPC has obtained significant consideration in the last decade [8, 9]. The geopolymers are developed under the chemical reaction of alumina-silicate mineral [10, 11], for instance, granulated blast furnace slag (GBFS), metakaolin (MK), fly ash (FA), and wheat straw ash (WSA), etc., with the alkaline activating chemical [12]. The activator assists in dissolving the glassy-shaped phases in the GBFS to create different solid phases, which include calcium-aluminate-silicate-hydrate, which primarily impacts the strength, microstructural and durability properties [13–15]. Ultra-high performance geopolymer concrete (UHPGPC) has advanced in the last decade [16, 17]. It is a new type of concrete with good compression, indirect tensile strength, a high proportion of binding material, and also lower water-to-binder ratio (w/b) [18, 19]. UHPGPC has materials that are small/fine in size to achieve proper dense concrete [20]. Highly dense geopolymer concrete can also yield excellent strength and durability [21]. The outflow of carbon dioxide is incessantly increasing every day due to the manufacturing of OPC [22, 23]. Research has been performed to diminish the usage of OPC and substitute it with other waste pozzolanic materials [24, 25]. Shi et al. [26] revealed that substituting 25% and 45% of OPC with FA and GBFS may increase the flexural strength of ultra-high-performance geopolymer concrete [27]. Spiesz et al. [28] reported that the mixture of UHPGPC was developed with a low dosage of OPC, resulting in a 25% decrease in the CO_2 outflow [29].

Moreover, Agwa et al. [30] revealed that substituting metakaolin and silica fume with a low proportion of OPC improved the strength of UHPGPC developed from the various discarded material. Compared with conventional concrete, geopolymer concrete is an appropriate substitute material for standard plain concrete, proving its worth in the practical field. Geopolymer materials [31] have a low price that could be developed with low energy and considerably minimum release of CO_2. Different researches concentrate on the durability characteristics of geopolymer concrete (GPC), whereas some evaluate the strength properties and functional attributes. He et al. [32] investigated the effect of the ratio of silica/alumina on the structural, strength properties, and chemical stability of geopolymer concrete with a molar ratio between 2 and 4 for the Silica/alumina ratio [33]. The authors also observed that the GPC with a four ratio of silica/alumina displayed significantly higher strength values than GPC with a two ratio of silica/alumina due to the high silica-oxygen-silica bond. Some researchers have studied the performance of geopolymer concrete with discarded materials as a partial/total replacement of fine or coarse aggregates or a binder. Haido et al. [34] employed discarded lime and scrapped glass as a fractional replacement for sand in geopolymer concrete. The findings depicted that the discarded lime and glass could be replaced in the formation of geopolymer concrete. Moreover, including 20% discarded glass reduced the compression strength at the curing of 7 and 28 days by 32.2% and 20.04%, respectively. Also, Ameri et al. [35] research is carried out to evaluate the optimal curing temperature and alkali activator to binder ratio of discarded

material added geopolymer mortar. The results showed that the compression and flexural strength were high when the curing heat was maintained at 90˚C, and the alkali activator to binder ratio was 0.55. Consequently, temperature curing is needed to develop GPC with suitable strength attributes. Youssf et al. [36] evaluated the strength behavior and durability of geopolymer concrete comprising rubber crumbs. The results showed that by adding 20% rubber crumbs as a fractional replacement of the fine aggregate, the fresh property was increased by 8%, water absorption was increased by 33%, loss in mass because of the degradation was improved by two times, drying shrinkage was increased by 30%. In contrast, the compression strength decreased by 29%, and the carbonation depth decreased by 16% [37].

Currently, the consideration of research has been on the formation of geopolymer concrete at ambient surroundings to lower the required energy for curing [38]. Regardless of the significant research in the geopolymer field, very little consideration has been given to developing ultra-high-performance geopolymer concrete with steel fibers and different waste materials. Iyer et al. [39] employed alumina-silicate materials (GBFS and silica fume) to make UHPGPC. The compression strength of UHPGPC with no steel fibers was 122 MPa, and when fibers were added, the compression strength improved to 173 MPa. Wetzel et al. [40] studied the impacts of silica fume on the fresh and strength characteristics of UHPGPC. The finding showed that even though UHPGPC doesn't comprise any OPC, it has excellent compression strength and low porosity, equivalent to standard ultra-high-performance concrete. The authors also revealed that the ultra-high-performance geopolymer concrete attained the highest compression strength of 181 MPa with 13% replacement of GBFS with silica fume. The fresh property was reported to get worse with the addition of 20% to 30% silica fume, which revealed that the silica fume significantly affects the fresh and strength properties of geopolymer concrete at a high replacement percentage. Althoey et al. [41] developed ultra-high-strength fiber-reinforced geopolymer concrete by substituting cement with nano-silica and activated with the alkaline activators and observed significant results.

Nonetheless, ultra-high-performance geopolymer concrete with no fibers could get brittle as the compression strength rises. Consequently, fibers of different types should be introduced to enhance the concrete's ductility [42–46]. Per Lao et al. [35], the maximum compression strength of UHPGPC was noted to be 221 MPa. With the high concentration of steel fibers, the compression strength of UHPGPC has risen because of the firm modulus of elasticity of fibers. The ultra-high-performance geopolymer concrete's tensile strength with a high percentage of steel fibers was also high because of the bridging behavior of fibers [47–50]. The findings displayed that geopolymer concrete could be the suitable answer for developing ultra-high-performance concrete with the most utilization of industrial discarded materials. It is being revealed that the mixtures with 16% and 32% of silica fume with the introduction of steel fibers could be highly appropriate for producing UHPGPC, as their compressive strength crosses the criteria of 125 MPa for being classified as ultra-high-performance concrete. Sammak et al. [51] have utilized polypropylene and steel fibers in UHPGPC. The results revealed that substituting a low percentage of steel fibers with polypropylene fibers reduces strength and improves the concrete's durability [52–57].

1.1 The novelty of current work

From the above literature, it can be noticed that no study utilizes different waste materials as a partial substitute for fine aggregate in developing ultra-high-performance geopolymer concrete (UHPGPC) with fibers. Therefore, the present research aims to establish that discarded materials (marble powder, waste rubber crumb powder, and waste glass) could be used as a fractional sand replacement in ultra-high-performance geopolymer concrete. This will assist

in conserving the natural river sand. The present study evaluates ultra-high-performance geopolymer concrete's fresh, strength and durability characteristics. For making ductile ultra-high-performance geopolymer concrete, double-hooked steel fibers were added. The results of the present study are also contrasted with the past research. Also, mercury intrusion porosimetry (MIP) analysis, thermogravimetric analysis (TGA), and x-ray diffraction (XRD) spectra were carried out to test the improvement of ultra-high-performance geopolymer concrete at the micro level.

2. Materials

2.1 Alkaline activators

Sodium silicate (Na_2SiO_3) and sodium hydroxide (NaOH) was employed as the alkali-activator chemicals. The ratio of Sodium silicate and sodium hydroxide was 3:1, the molarity of sodium silicate was 2M, and sodium hydroxide molarity was 10M. These chemicals were procured from the Islamabad chemical factory and were 99.9% pure.

2.2 Binders

As presented in Fig 1A and 1B, granulated blast furnace slag (GBFS) and wheat straw ash (WSA) were used as geopolymer binders. The surface area and specific gravity of WSA and GBFS were 16500 m^2/kg, 2.24, and 376 m^2/kg, 2.84, respectively. The GBFS was procured from heavy industries Taxila, and WSA was obtained from the commercial market in Islamabad. The x-ray diffraction (XRD) for the GBFS and WSA is also presented in Figs 2 and 3.

2.3 Used waste materials (waste rubber powder, glass waste, and marble waste)

Waste tire rubber was acquired from the local supplier, and it was grinded to a very fine size (< 4.75 mm) to make waste rubber powder (WRP), as presented in Fig 4A. Waste rubber powder, glass waste and marble waste had a density of 1114, 2725, and 2675 kg/m^3. Glass waste (GW) and marble waste (MW) were obtained from a local glass and marble manufacturer in Mardan. It was also grinded to very fine pieces, as presented in Fig 4B and 4C. The specific gravity of waste rubber powder, glass waste, and marble waste were 1.2, 2.4, and 2.6. The

Fig 1. (a) GBFS; (b) WSA.

https://doi.org/10.1371/journal.pone.0285692.g001

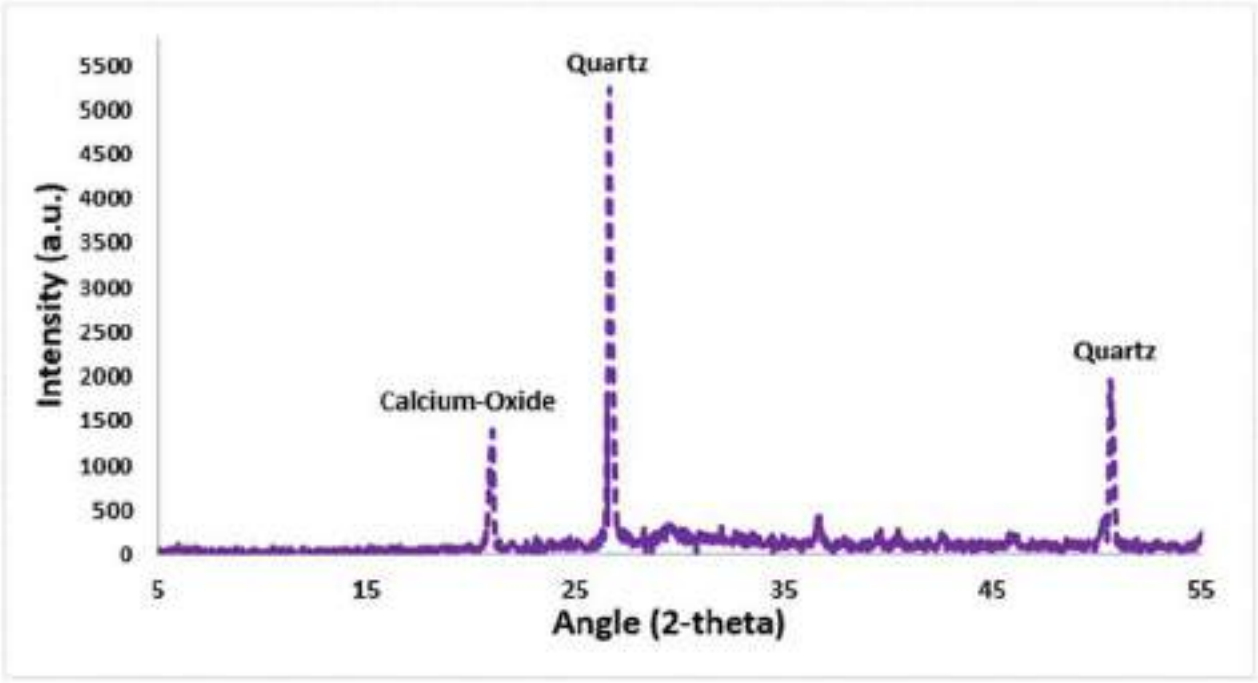

Fig 2. XRD analysis of Wheat Straw Ash (WSA).

https://doi.org/10.1371/journal.pone.0285692.g002

granulometry curve of WRP, GW, MW and fine aggregate is presented in Fig 4D. The chemical composition of WRP, GW, and MW is presented in Table 1.

2.4 Steel fibers

Length and the aspect ratio of steel fibers are critical, which govern the effectiveness of the strength characteristics of concrete. The past study revealed that adding 25 to 50 mm fibers optimally enhances the strength characteristics [58]. Thus, in the present research, double-hooked end steel fibers were used, as shown in Fig 5, with a length of 50 mm and a diameter of 1.15 mm. The steel fibers were obtained from the commercial market in Lahore, and their physical characteristics are provided in Table 2.

2.5 Fine aggregates

The fine aggregates (sand) were procured from Nowshera's river bank. Fine aggregate's specific gravity and density were 2.70 and 1585 kg/m^3. The size of fine aggregates was kept at less than 4.75 mm.

3. Preparation of concrete specimens

In the present study, ten different mixtures were developed. All the mixtures had a constant percentage of steel fibers by the volume of the binder. In the first mix, no waste rubber powder, glass waste, or marble waste was added to the mixture, and it had only alkaline activator solution, granulated blast furnace slag, wheat straw ash, natural coarse aggregates, fine aggregates (sand), water, and 2% steel fibers. The second, third, and fourth mixes had 5%, 10%, and 15% waste of rubber powder, glass waste, and marble waste by weight. The binder ratio (GBFS/WSA) was kept at 2.33. According to the literature [30, 40, 59], adding silica fume (SF) is

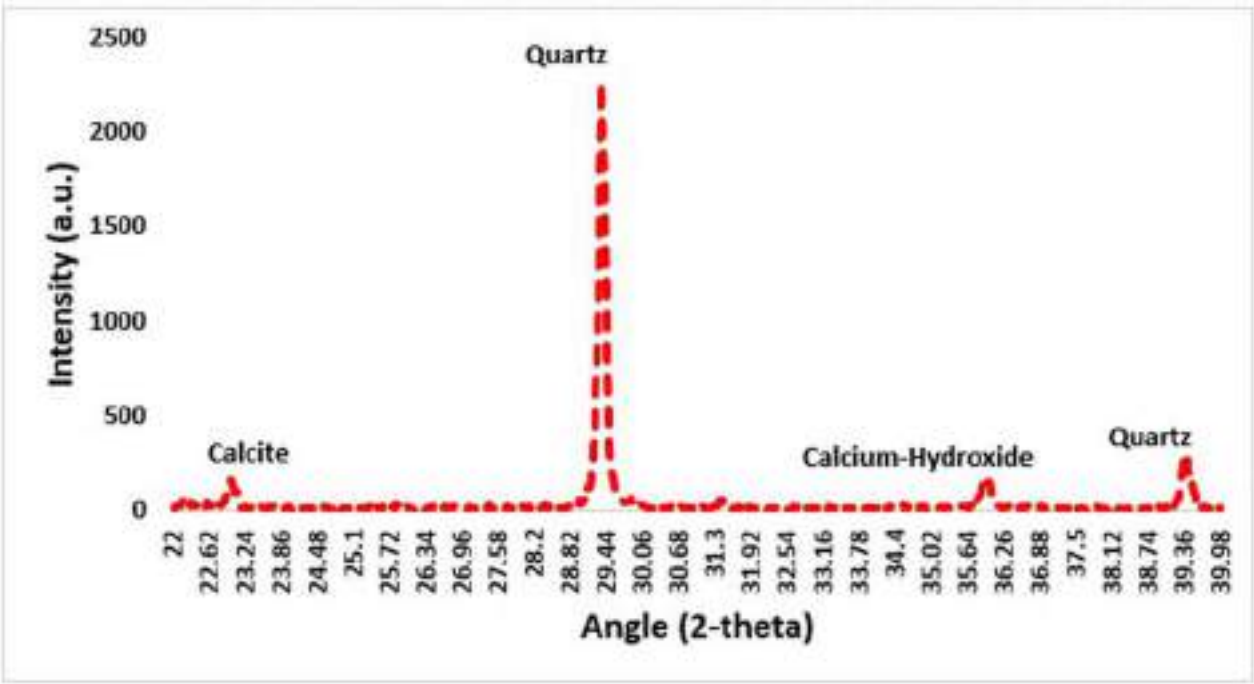

Fig 3. XRD analysis of Granulated Blast Furnace Slag (GBFS).

https://doi.org/10.1371/journal.pone.0285692.g003

necessary to develop ultra-high-performance concrete. The ratio of the alkaline-activator solution to the alumina-silicate of the tried sample is fixed at 0.40 (based on the findings of strength properties discussed below). Table 3 shows the complete mix details of all samples.

To prepare an alkaline-activator solution, sodium-hydroxide was first added to water. Due to an exothermic reaction, it was left undisturbed for 24 hours to obtain the ambient temperature. A sodium silicate chemical was added to it. All the dry materials were mixed in a mechanical mixer for four minutes to make ultra-high-performance fiber-reinforced geopolymer concrete. Then slowly, the alkaline-activator solution was introduced to the mix and mixed for 3 minutes. Then 50% water with steel fibers was introduced to the mixer and slowly blended for two minutes to ensure the proper orientation of fibers in the mix. As the mixture started to have a uniform color, the remaining 50% water was introduced to the mechanical mixer. Lastly, the freshly mixed concrete was poured into plastic molds and kept air-tight to prevent moisture loss. After one day, the concrete was de-molded, and the concrete samples were placed in the curing tank [33]. The terminology for mix ID is designed so that M1, M2, and M3 represent three different groups of modified mixtures. The number after the GW, MW, and WRP shows the percentage of material added to that modified mixture. Three samples for each combination were tried to prevent variability in the test results, and its average value was considered the final value. So, the result values provided in all Figures are the average values.

The concrete samples were tried at 7, 28 and 90 days when their casting was completed. The impact of curing on the compression strength was studied following four significant types of curing (ambient curing [24], water curing, autoclave curing at 85˚C for 24 hours, and temperature curing at 75˚C for 24 hours). The samples were put in the lab under room conditions for ambient curing. The ambient and water curing were done at 28 days. When the 28 days were completed, half of the ambient cured samples were placed in an oven at 75˚C for twenty-

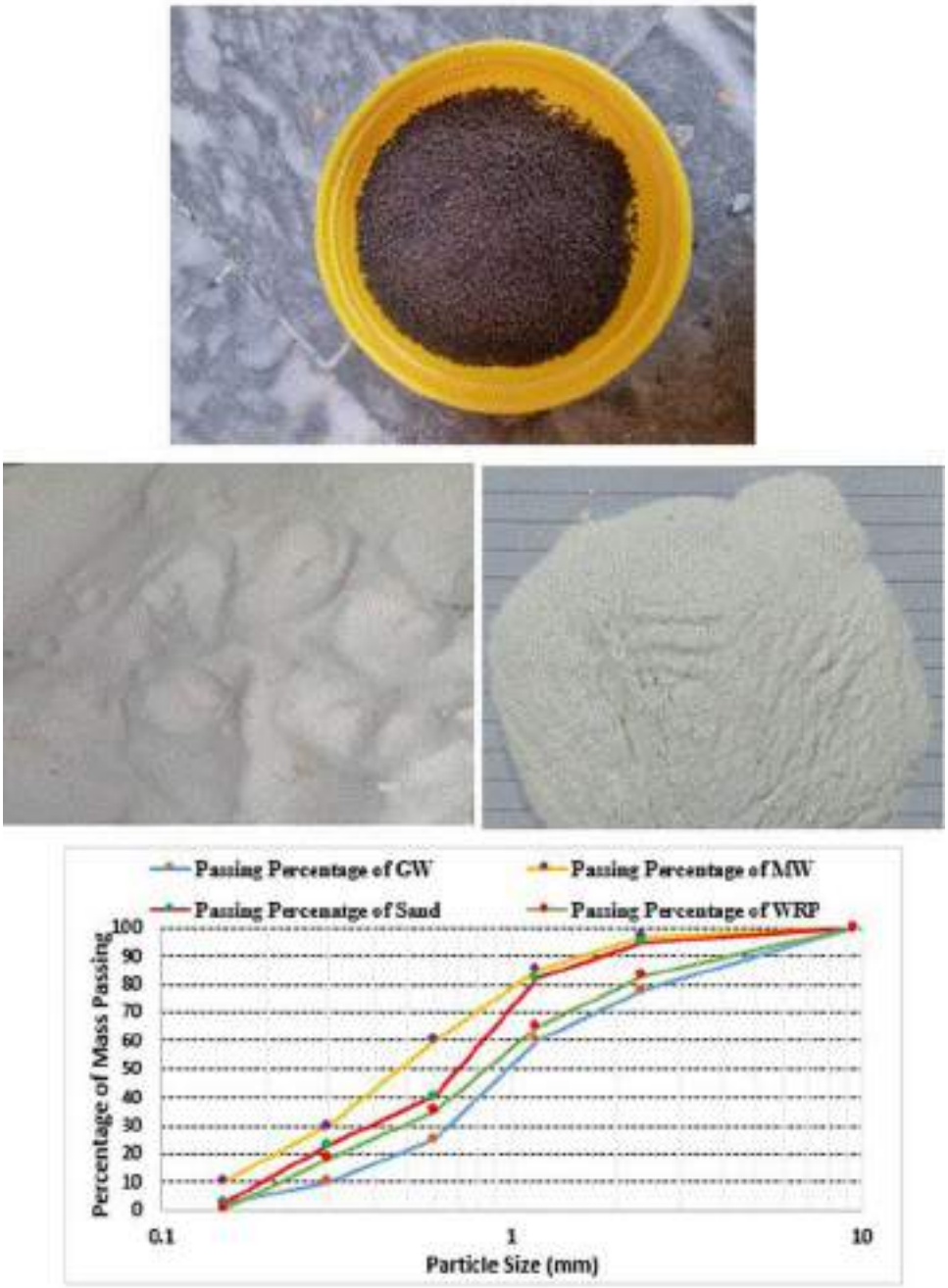

Fig 4. Waste materials in grinded form; (a) Waste rubber powder, (b) Glass waste powder, (c) Marble waste powder, (d). Granulometry curve of WRP, GW, MW and fine aggregate.

https://doi.org/10.1371/journal.pone.0285692.g004

four hours, whereas the remaining samples were placed in the autoclave to study the impact of the heating condition on the compression strength of UHPGPC.

Table 1. Chemical composition of WRP, GW, and MW.

Component	WRP (%)	GW (%)	MW (%)
Silicon Dioxide (SiO_2)	5	71	4
Aluminum Oxide (Al_2O_3)	1	2	2
Calcium Oxide (CaO)	1	7	51 (as $CaCO_3$)
Magnesium Oxide (MgO)	0	3	31 (as $MgCO_3$)
Sodium Oxide (Na_2O)	1	12	6
Potassium Oxide (K_2O)	0	2	1
Carbon Black	29	0	0
Polymeric materials (e.g., SBR)	54	0	0
Fillers and additives	7	0	0
Iron Oxide (Fe_2O_3)	1	1	2
Other trace elements and compounds	1	2	3

https://doi.org/10.1371/journal.pone.0285692.t001

4. Characterization of tests

4.1 Fresh properties of UHPGPC

The flowability of freshly mixed UHPGPC was assessed following ASTM C1437 [60]. Per ASTM C191 [61], the setting time of freshly mixed concrete was evaluated. The concrete's unit weight conformed with ASTM C138.

4.2 Strength properties of UHPGPC

The compression and the indirect tensile strength of UHPGPC were evaluated with the universal testing machine (UTM) with a capacity of 1500 kN. The loading rate for the indirect tensile strength was 0.15 MPa/sec, and for the compression strength, the loading speed was 1.5 MPa/sec. For every mixture of UHPGPC, three sets of the same samples were prepared and tried at 7, 28, and 90 days, and the average value was used to decrease the experimental error. The compression strength was evaluated per ASTM C39 [62] on cylindrical concrete samples with

Fig 5. Double-hooked end steel fibers.

https://doi.org/10.1371/journal.pone.0285692.g005

Table 2. Physical characteristics of double hooked end steel fibers.

Physical Characteristics	Value
Length of steel fiber	50 mm
Diameter (d)	1.15 mm
Tensile Strength	2235 N/mm^2
Aspect ratio (l/d)	43.47
Hook depth	1.25 mm
Hook length	1.5–3 mm

https://doi.org/10.1371/journal.pone.0285692.t002

12 inches x 6 inches (length x diameter). The direct transmission technique assessed the ultrasonic pulse velocity (UPV) at 28 days on a 50 mm cubic sample. The indirect tensile strength of UHPGPC was determined following ASTM C496 [63]. The modulus of elasticity and flexural strength of UHPGPC was determined following ASTM C469 [64] and ASTM C78 [65]. Concrete beams of 30 mm x 30 mm x 150 mm were developed and tested.

4.3 Durability properties of UHPGPC

Rapid chloride penetration tests (RCPT) were performed per ASTM C1202 [66], and three specimens of 50 mm were arranged. After the saturation in water, the specimens were positioned in the instrument cell for testing them. The specimens were in contact with a 0.2 molar solution of NaOH on one side and with 2% of NaCl on another side. By passing a volt of 65, the current travelling over the specimen was measured in five hours. The total current travelling over the specimen was measured in (Coulombs).

To evaluate the electrical resistivity (ER) of UHPGPC, electrodes were placed on both sides of the specimen, and the passing voltage was measured. The ER can be measured by following Eq (1). The concrete's surface should be horizontal to ensure a thorough connection between the specimen and the electrode. Cube-size specimens were utilized for the measurement of ER.

$$\boldsymbol{\rho} = \boldsymbol{A} * \frac{(\mathbf{R})}{(\mathbf{L})} \tag{1}$$

In equation (A), R is the resistance during the test, ρ is the specific electrical resistance (ohm. Meter), L is the specimen's length, and A is the x-section area over which the charges travel (m^2).

4.4 Microstructural study of UHPGPC

To assess the development of crystalline phases in the UHPGPC, x-ray diffraction (XRD) spectra were done. The XRD analysis was done with a passing current of 35 milli-Ampere and a voltage of 35 kilo-Volt. Thermogravimetric analysis (TGA) was employed to determine the loss in mass of hardened UHPGPC, dehydration and degradation due to wear and tear. TGA was performed at the heating rate of 15˚C/minute with temperatures ranging from 30˚C to 900˚C. The concrete's porosity was evaluated utilizing the mercury intrusion porosimetry (MIP) method. The concrete samples were cut into smaller portions of 15 mm x 15 mm x 30 mm from the 30 mm x 30 mm x 150 mm samples.

Table 3. Mix proportion of all concrete mixtures (kg/m^3).

Mix ID	WSA	GBFS	SF	FA	GW	MW	WRP	DHSF	NaOH	SS	Water
Control	201	469	155	1060	0	0	0	15.5	68	204	145
M1-GW-5	201	469	155	107	78	0	0	15.5	68	204	145
M1-GW-10	201	469	155	954	139	0	0	15.5	68	204	145
M1-GW-15	201	469	155	901	192	0	0	15.5	68	204	145
M2-MW-5	201	469	155	107	0	78	0	15.5	68	204	145
M2-MW-10	201	469	155	954	0	139	0	15.5	68	204	145
M2-MW-15	201	469	155	901	0	192	0	15.5	68	204	145
M3- WRP -5	201	469	155	107	0	0	78	15.5	68	204	145
M3- WRP-10	201	469	155	954	0	0	139	15.5	68	204	145
M3-WRP-15	201	469	155	901	0	0	192	15.5	68	204	145

WSA–Wheat straw ash, **GBFS**–Granulated blast furnace slag, **FA**–Fine aggregate, **GW**–Glass waste, **MW**–Marble waste, **WRP**–Waste rubber powder, **DHSF**–Double hooked steel fiber, **NaOH**–Sodium hydroxide.

https://doi.org/10.1371/journal.pone.0285692.t003

5. Results and discussion

5.1 Fresh characteristics of UHPGPC

Fig 6A and 6B presents the impact of the substitution of waste materials on the initial and final setting time and flowability of UHPGPC. No segregation or bleeding was observed in the fresh mix when performing the fresh test. As observed from Fig 6A, the flowability of UHPGPC is significantly affected by the existence of waste rubber powder (WRP), glass waste (GW), and marble waste (MW). It could also be noted that the concrete's flowability was raised with the addition of GW, and the flowability increased when the percentage of GW was increased. This could be ascribed to the glass material's low water absorption capability and lower friction coefficient of GW, which increase the flow rate. Hence, the flowability of UHPGPC with no WRP, GW, and MW was 216 mm, and its rise correspondingly by 2.1%, 3.9%, and 4.42% with the addition of 5%, 10%, and 15% glass waste in the concrete's mixtures. Wetzel et al. [4] also revealed similar results when evaluating fresh properties of ultra-high-performance geopolymer concrete. When the sand was substituted by marble waste (MW) by 5%, 10%, and 15%, the concrete's flowability was reduced by 4.07%, 7.32%, and 9.21%, respectively, when contrasted with the reference mixture. Also, the UHPGPC's flowability was reduced when the percentage of waste rubber powder (WRP) was increased. Hence, the addition of 15% WRP had the lowermost flowability, which could be attributed to the high coefficient of friction and hydrophobic behavior of rubber material, which augments the resistance against the flow. As presented in Fig 6B, it can be noted that the mixtures with the GW usually increase the initial and final setting time by 18% and 12%, respectively, with the utilization of 15% GW in the mixtures when compared with the reference mixture. Moreover, marble waste (MW) has considerably decreased the flowability with a low initial and final setting time, signifying that the combination of marble particles has a favorable impact in accelerating the process of geo-polymerization. The hydrophilic behavior and coefficient of high friction of rubber particles led to frail bonds amid the rubber elements and geopolymer gel. Hence, the flowability of UHPGPC deteriorates with the utilization of WRP; also, it had the highest initial and final setting time.

5.2 Hardened characteristics of UHPGPC

5.2.1 Density. The density of ultra-high-performance geopolymer concrete was calculated at curing 28 days, as presented in Fig 6C. It could be noted that the addition of glass waste had

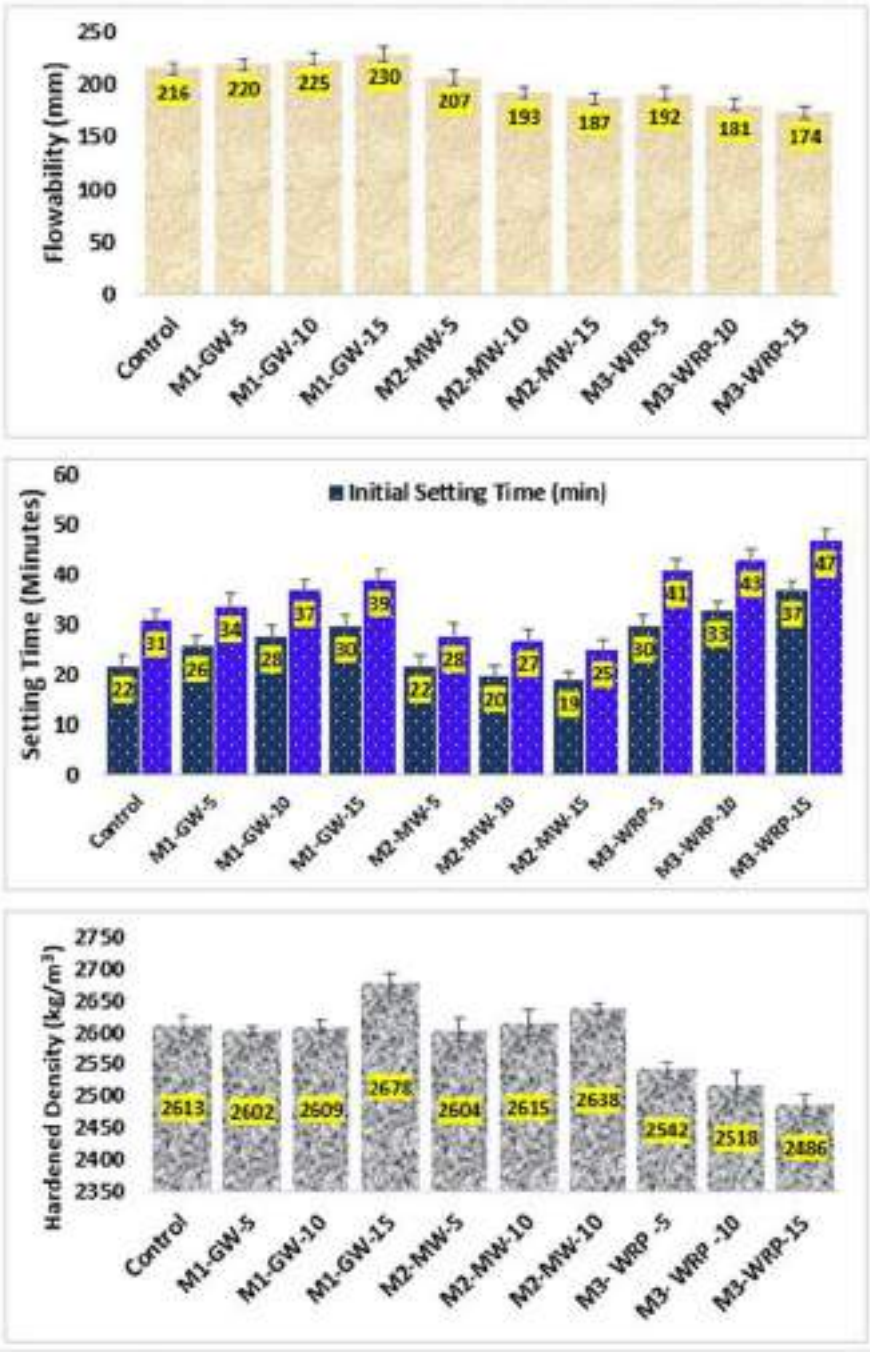

Fig 6. (a) Slump flow (mm) of UHPGPC, (b) Initial and final setting time of UHPGPC, (c) Hardened density of concrete.

https://doi.org/10.1371/journal.pone.0285692.g006

the maximum unit weight compared to the reference mixture, which can be ascribed to the high-water absorption of glass waste. Employing glass waste as a replacement also had the same effect on the concrete density as it was higher than the reference mixture; this could be ascribed to the improved inherent properties of GW and low water absorption.

The reason glass waste higher hardened density than other mixtures is because of the differences in the physical and chemical properties of these waste materials. Glass waste is a non-porous material that has a high packing density and can improve the particle packing of the concrete, resulting in a higher density and stronger concrete [40]. Additionally, glass waste can react with the geopolymer binder, contributing to the strength and durability of the UHPGPC. On the other hand, waste rubber powder and marble waste are porous materials that may have lower packing densities than glass waste [67]. The porous nature of these materials may also lead to weaker interfaces between the waste particles and the geopolymer binder, resulting in a lower strength UHPGPC. Additionally, waste rubber powder and marble waste may not react with the geopolymer binder as effectively as glass waste, leading to a weaker UHPGPC. Increasing the percentage of glass waste in UHPGPC can lead to a higher hardened density due to the increased amount of non-porous material present in the mixture. Specifically, adding 15% glass waste to UHPGPC can result in a higher hardened density than adding only 5% or 10% glass waste. This may be due to the optimal packing density and amount of silicate in the mixture. In comparison, the inclusion of WRP reduced the density because of the low unit weight of rubber and its hydrophilic properties. The evaluated density of ultra-high-performance geopolymer concrete ranged from 2486 kg/m^3 and 2675 kg/m^3.

5.2.2 Ultra-Sonic Pulse Velocity (UPV). UPV is a non-destructive testing method for evaluating the strength of concrete [68]. This test was performed on the concrete samples cured at 7, 28 and 56 days, and its test outcomes are presented in Fig 7. The utilization of GW raised the ultras-sonic pulse velocity, whereas the inclusion of marble waste lowered the UPV. When contrasted with the mixtures comprising GW, the UPV of MW mixtures was lowered

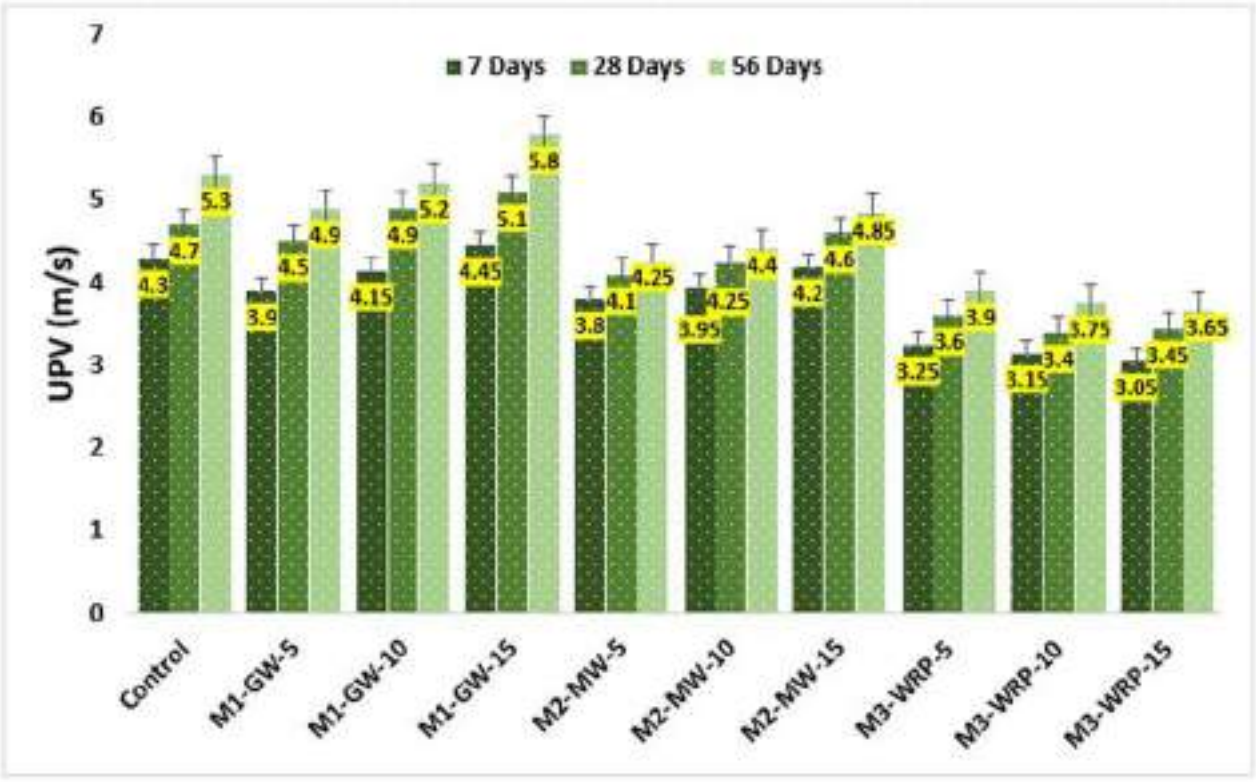

Fig 7. Ultra-Sonic Pulse Velocity (UPV) of UHPGPC.

https://doi.org/10.1371/journal.pone.0285692.g007

by 10.5%. With the introduction of waste rubber powder, the UPV of UHPGPC was reduced significantly (20.14%) with the reference mixture. The increasing values in the ultrasonic pulse velocity (UPV) test of ultra-high-performance geopolymer concrete (UHPGPC) upon the addition of waste rubber powder (WRP), glass waste (GW), and marble waste (MW) as partial substitutes for fine aggregate can be attributed to several factors. Incorporating these waste materials, particularly GW and MW, may lead to a denser microstructure due to their fine particle sizes, which can fill the voids and improve particle packing. The pozzolanic reactivity of GW and MW can also contribute to forming additional geopolymer products, which can further refine the pore structure and enhance the concrete's overall performance [69]. While WRP does not have pozzolanic properties, its addition can improve the overall particle packing and distribution within the matrix. Consequently, the denser and more refined microstructure increases the UPV values, indicating improved homogeneity and quality of the UHPGPC. This also happened due to the mixtures' enhanced porosity comprising WRP compared to the mix with only fine natural aggregates. The sound waves travel over solid material more quickly than porous material. The ultrasonic pulse velocity values conform with the compression strength of UHPGPC.

5.2.3 Compressive strength. The compressive strength of ultra-high-performance geopolymer concrete at the curing of 7, 28, 56, and 90 days is presented in Fig 8. As anticipated, the compressive strength of UHPGPC was impacted by the addition of WRP, GW, and MW. At 15% substitution of GW, the maximum compressive strength of 179 MPa was noted at the curing of 90 days, while the control sample had a compressive strength of 161 MPa at 90 days. The compressive strength of UHPGPC at 90 days was observed to reduce to 120 MPa as the 15% WRP was added. Adding 5% glass waste increased the strength after 56 days of curing compared to the control mixture, from 150 MPa to 154 MPa. Per past studies, when glass waste is employed to replace sand, the compressive strength rises as the percentage of GW is enhanced. Also, the compressive strength of UHPGPC at 15% GW reached 159 MPa and 179 MPa at 56 and 90 days, respectively. It is also noted that the concrete with 15% GW had more compression strength compared to 5% GW and 10% GW by 6.14% and 4.46% at 90 days. The higher compressive behavior of the samples with GW was ascribed to the dense matrix in which the shapeless SiO_2 in a glass particle integrates with the geopolymer matrix and shows considerable phases of calcium-aluminate-silicate-hydrate products. This enhancement can be attributed to the pozzolanic activity of the fine glass waste particles, which react with the alkaline activators in the geopolymer matrix, forming additional geopolymer products. Consequently, a denser and more refined microstructure is achieved, contributing to increased compressive strength. The 15% glass waste replacement demonstrated superior compressive strength compared to the 5% and 10% replacements, suggesting an optimal balance between the particle packing and the pozzolanic activity of the glass waste. This balance maximizes the benefits of the glass waste's inclusion while maintaining adequate workability and overall performance [70, 71].

At 15% substitution, MW had 140 MPa, 145 MPa, 153 MPa, and 172.5 MPa at the curing of 7, 28, 56, and 90 days. Also, a negative influence on the compressive strength was noted as the amount of WRP was raised in the mixtures. The strength degradation in the concrete with WRP could be ascribed to the hydrophobic behavior and high coefficient of friction of the WRP, which forms weak bonds amid rubber elements and gel of geopolymer, and increased permeability, which leads to low-dense microstructure. Hence, employing 15% WRP reduces the compressive strength by 25.46% (120 MPa) at 90 days compared to the reference mixture. From Fig 9A and 9B, it could be noted that the concrete with 15% glass waste failed vertically in both directions, which shows the homogeneity and strong bond of steel fibers in the UHPGPC's matrix. In contrast, the concrete with 15% waste rubber powder was cracked

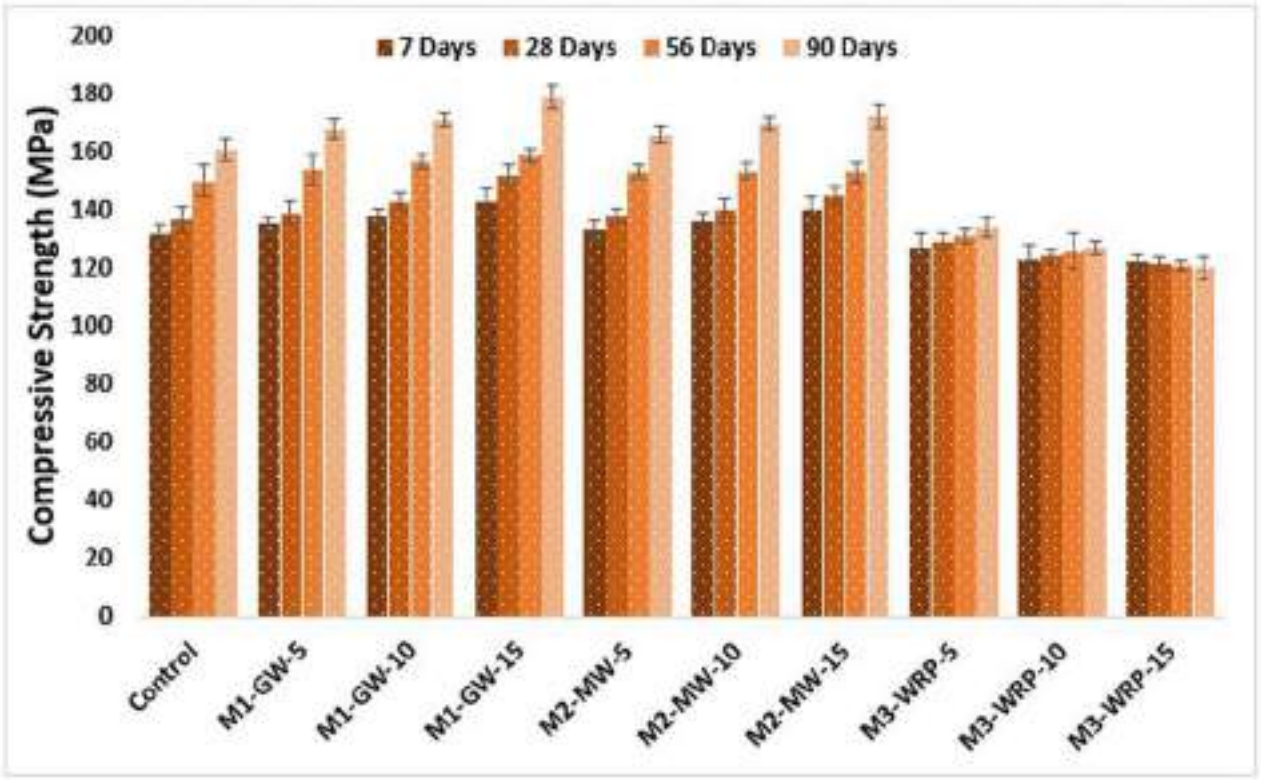

Fig 8. Compressive strength of UHPGPC at 7, 28, 56, and 90 days.

https://doi.org/10.1371/journal.pone.0285692.g008

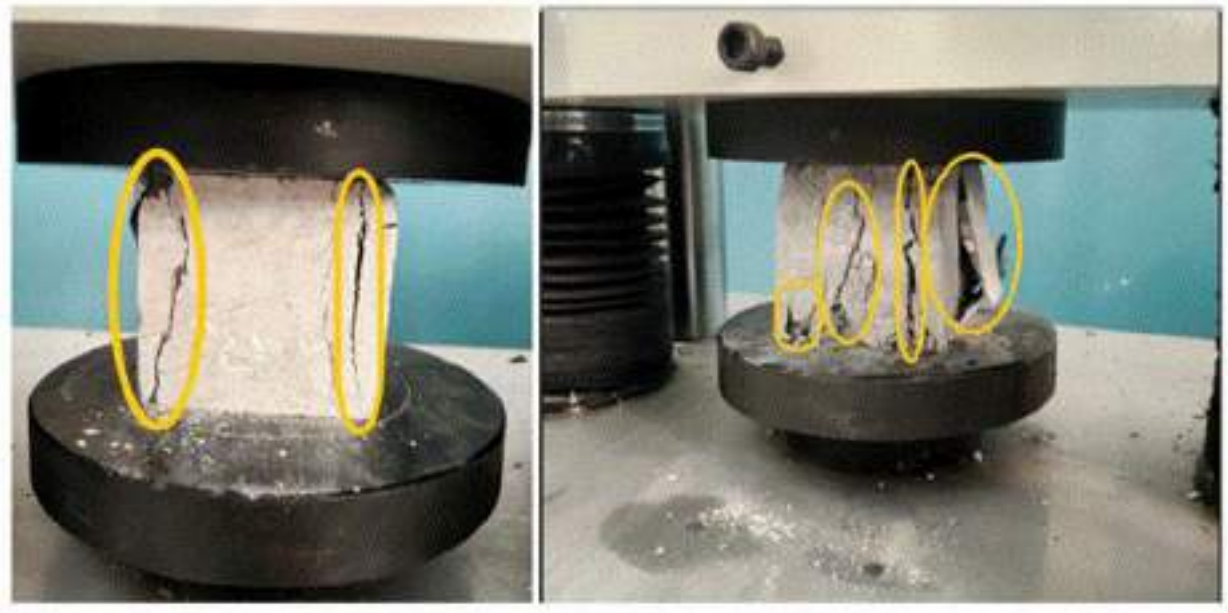

Fig 9. Failure patterns of UHPGPC under compression load; (a) M1-GW-15, (b) M3-WRP-15.

https://doi.org/10.1371/journal.pone.0285692.g009

entirely and failed in every direction when loaded in compression. This signifies the heterogeneity of the concrete's matrix that the steel fibers couldn't bond with the rest of the materials thoroughly. It is worth noting that the differing properties of waste materials can impact compressive strength. Marble waste and waste rubber powder do not exhibit the same pozzolanic reactivity as glass waste, potentially resulting in a less refined microstructure and inferior compressive performance. The presence of double-hooked end steel fibers in UHPGPC also plays a significant role in enhancing compressive strength. These fibers provide mechanical interlocking and improved load transfer, increasing cracking and deformation resistance under compressive loads [34, 72]. The optimal performance observed with the 10% glass waste replacement could be due to a synergistic effect between the improved glass waste microstructure and the steel fibers' reinforcing properties.

Fig 10 depicts the concrete's compressive strength under various curing techniques, which aligns with past studies [73]. It could be observed that autoclave and heat curing improved compressive strength. The selection of curing impacts the compressive strength, the response of steel fibers to the GPC's mix and the reaction between binders [74]. Autoclave curing enhances the concrete's microstructure and geo-polymerization extent [75]. Consequently, increasing the heat curing enhances the compressive strength. Significantly, autoclave and thermal curing improved the compressive strength, with enhancements of 7.14% and 11.51% of the curing under room temperature. It was also observed that as the percentage of GW increased, the molar ratio of CaO/SiO_2 and SiO_2/Al_2O_3 was noted in UHPGPC. The molar ratio of calcium oxide/silica and silica/alumina is associated with hydration products, such as calcium-silicate-hydrate and calcium-aluminate-silicate-hydrate. A rise in the molar ratios of

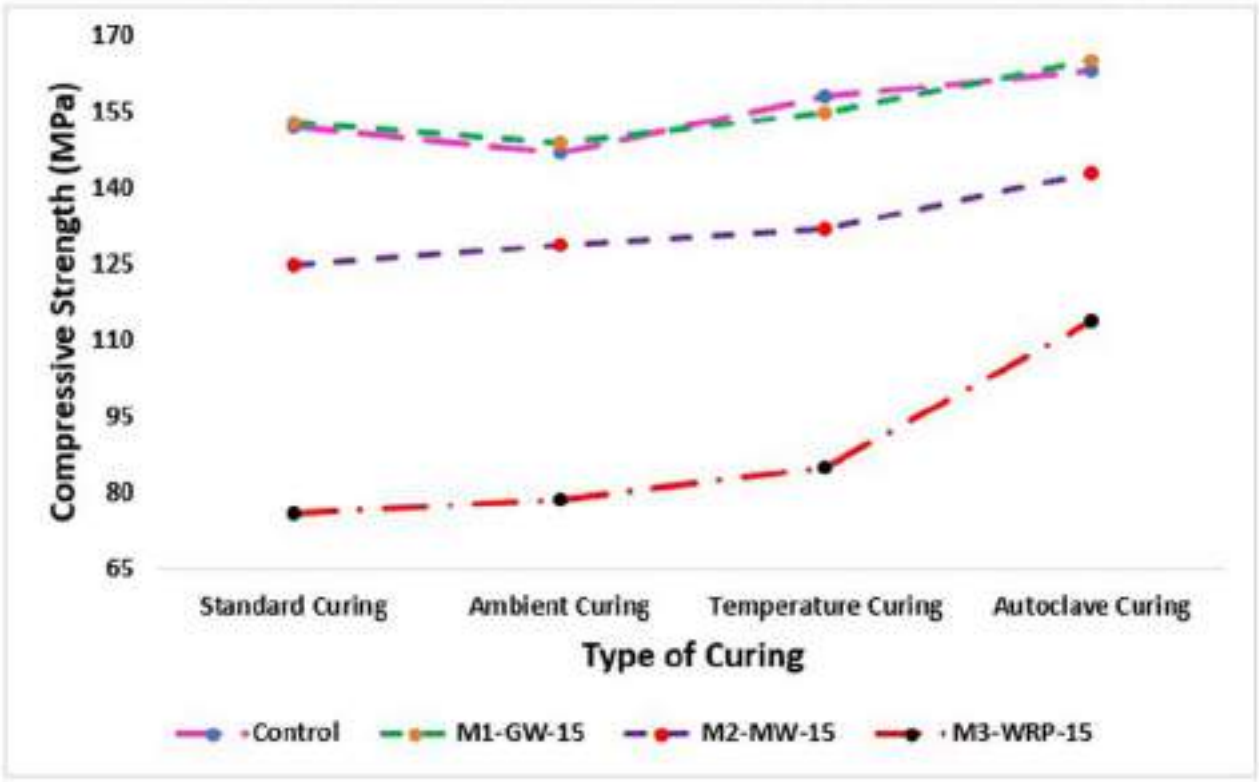

Fig 10. Effect of type of curing on compressive strength of UHPGPC.

https://doi.org/10.1371/journal.pone.0285692.g010

calcium oxide/silica and silica/alumina led to additional gels of calcium-silicate-hydrate and calcium-aluminate-silicate-hydrate, which leads to dense microstructure [76].

5.2.4 Modulus of elasticity (MOE). Fig 11 presents the results of MOE of the ultra-high-performance geopolymer concrete mixtures and their relationship with the compression strength. Glass waste particles are generally more angular and possess a wider size distribution, which can lead to better inter-particle bonding and enhanced packing within the geopolymer matrix. Results show that the 15% glass waste replacement demonstrated a higher modulus of elasticity than the 5% and 10% replacements. This outcome suggests that the higher glass waste content promotes a more effective particle packing within the matrix, contributing to a stiffer and more robust structure capable of resisting deformation under applied loads. It was noted that adding WRP, GW, and MW as a substitute for sand impacts the mixture's MOE. As the proportion of glass waste increased, the elasticity modulus was reduced. The modulus of elasticity M1-GW-5, M1-GW-10, and M1-GW-15 was 1.19%, 10.34%, and 13.52% lesser than the reference mixture. In the present study, the control sample's mean MOE and compressive strength at 28 days was 31.7 GPa and 152 MPa. Tayeh et al. [77] studied the UHPGPC's MOE and noted that the modulus of elasticity and compression strength were 43 GPa and 178 MPa, respectively. At 15% substitution of WRP, GW, and MW, the MOE was reduced by 21.24%, 12.35%, and 21.56% compared to the reference mixture. It is important to consider that marble waste and waste rubber powder have different particle shapes and size distributions compared to glass waste, which could affect the modulus of elasticity. These materials' less favorable packing characteristics might result in a less stiff geopolymer matrix, leading to a lower modulus of elasticity [78, 79].

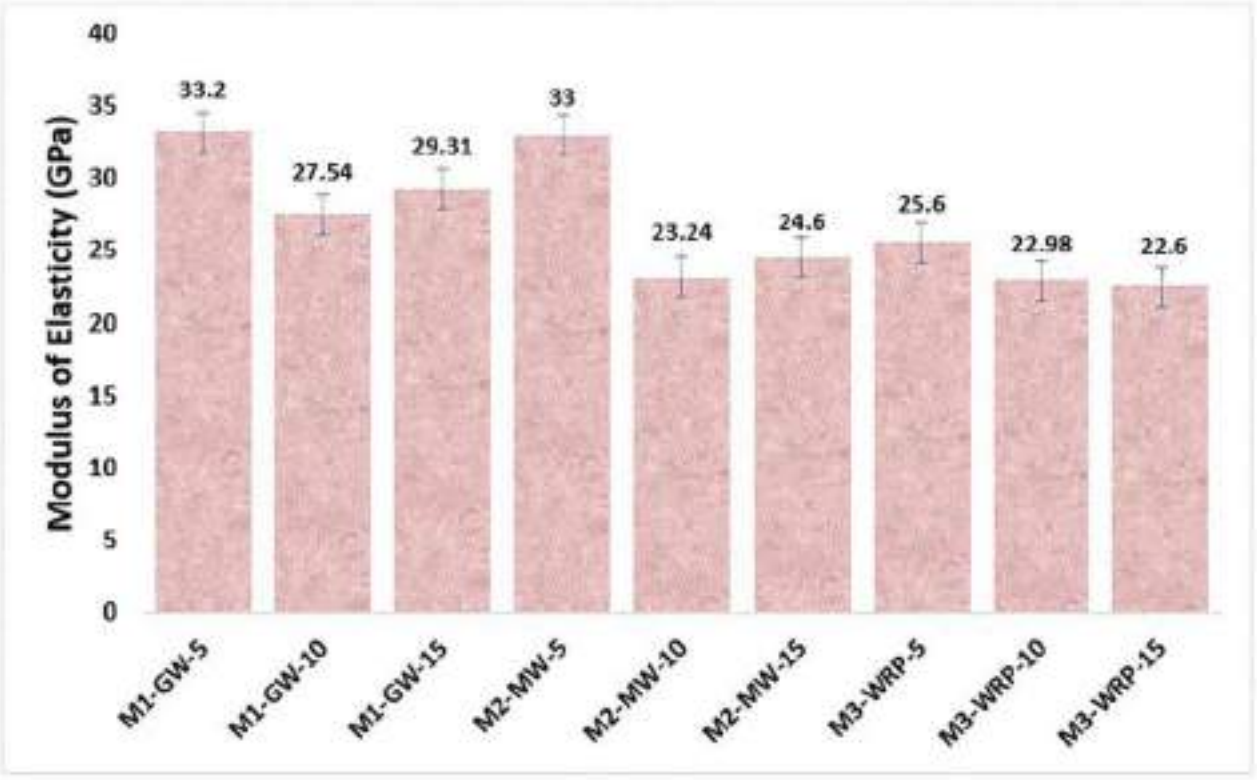

Fig 11. Modulus of elasticity of UHPGPC at 28 days.

https://doi.org/10.1371/journal.pone.0285692.g011

Additionally, double-hooked end steel fibers in UHPGPC are crucial in improving the modulus of elasticity [51, 80]. The steel fibers form a continuous network throughout the geopolymer matrix, enhancing load transfer and reducing the strain developed under loading conditions. The superior performance observed with the 15% glass waste replacement might be attributed to the combined effect of the improved particle packing and the reinforcing action of the steel fibers. The relationship between MOE and compression strength conformed with the analytical relationship developed by Tayeh et al. [77].

5.2.5 Indirect tensile strength. Fig 12 presents the influence of the different percentages of WRP, GW, and MW on the indirect tensile strength of ultra-high-performance geopolymer concrete at 28 and 90 days. The indirect tensile strength of ultra-high-performance geopolymer concrete (UHPGPC) at 28 and 90 days exhibited noticeable improvement with the incorporation of glass waste compared to marble waste and waste rubber powder. When evaluating the effects of various glass waste replacement levels, the 15% substitution displayed excellent indirect tensile strength compared to both the 5% and 10% replacements. With increasing the percentage of GW from 0% to 15% at 5% intervals, the indirect tensile strength reduced by 5.66%, 4.5%, and 2.41% at 28 days and 6.53%, 5.93%, and 3.13% at 90 days of curing, correspondingly. This low reduction in the indirect tensile strength of UHPGPC can be attributed to the pozzolanic activity of the fine glass waste particles, which react with the alkaline activators in the geopolymer matrix, creating additional geopolymer products. The formation of these products leads to a denser and more refined microstructure, ultimately contributing to increased strength. Despite these improvements, the control mixture without glass waste still demonstrated higher indirect tensile strength than all modified mixtures [10, 81]. This

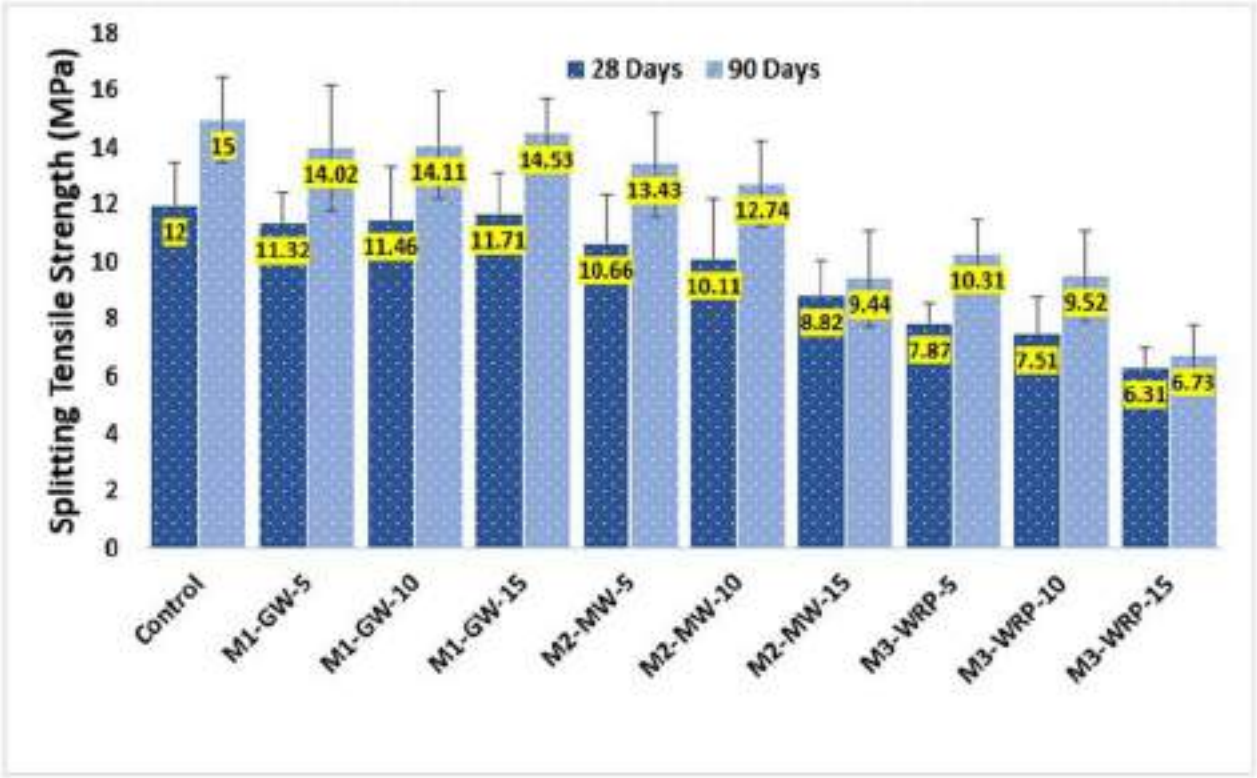

Fig 12. Indirect tensile strength of UHPGPC at 28 and 90 days.

https://doi.org/10.1371/journal.pone.0285692.g012

outcome may be due to the superior mechanical interlocking and load transfer provided by the double-hooked end steel fibers, which were more effective in the control mixture. The presence of steel fibers in the UHPGPC contributes to the overall tensile performance and crack resistance, playing a significant role in the observed strength differences between the control and modified mixtures [82, 83].

Moreover, when increasing the marble waste from 0% to 15% at 5% intervals, the split tensile strength was reduced by 11.16%, 15.75%, and 26.5% at 28 days and 10.46%, 9.12%, and 33.09% at 90 days of curing, respectively, compared with the reference sample. When waste rubber powder was added from 0% to 15% at 5% intervals, the indirect tensile strength was reduced by 34.41%, 33.65%, and 44.93% at 28 days and 29.04%, 29.11%, and 47.17% at 28 and 90 days of curing, respectively, compared with the control sample. From Fig 13A and 13B, it can be observed that the sample with 15% glass waste was cracked in multiple positions, which shows the better bonding of steel fibers with the glass waste and geopolymer gel. In contrast, the sample with 15% WRP failed wide open only in one direction when an external loaded was applied, which shows the poor bonding of WRP with the steel fibers and concrete's matrix. The reduction in concrete's strength due to the addition of WRP was ascribed to the weak bonding between geopolymer gel and the rubber elements [84]. Furthermore, the contrasting properties of the waste materials could have also impacted the tensile strength. Marble waste and waste rubber powder, for instance, do not exhibit the same pozzolanic reactivity as glass waste, potentially leading to a less refined microstructure and mediocre properties.

5.2.6 Flexural strength. Fig 14 depicts the flexural strength of ultra-high-performance geopolymer concrete with different discarded materials at the curing of 28 and 56 days. The flexural strength ranged from 4.85 MPa to 12.62 MPa. It is noted that raising the percentage of glass waste helped to enhance the concrete's flexural strength. This improvement could be ascribed to the silica reaction from the glass material with an alkaline-activator solution that augments the concrete's microstructure [85]. Hence, with the increasing percentage of glass waste from 5% to 15%, the flexural strength improved by 3.56%, 5.96% (at 5% GW), 4.73%, 6.31%, (at 10% GW), and 6.89%, 8.03%, (at 15% GW), respectively, compared with the reference mixture of 11.90 MPa and 13.4 MPa at 28 and 90 days of curing. Concerning the control

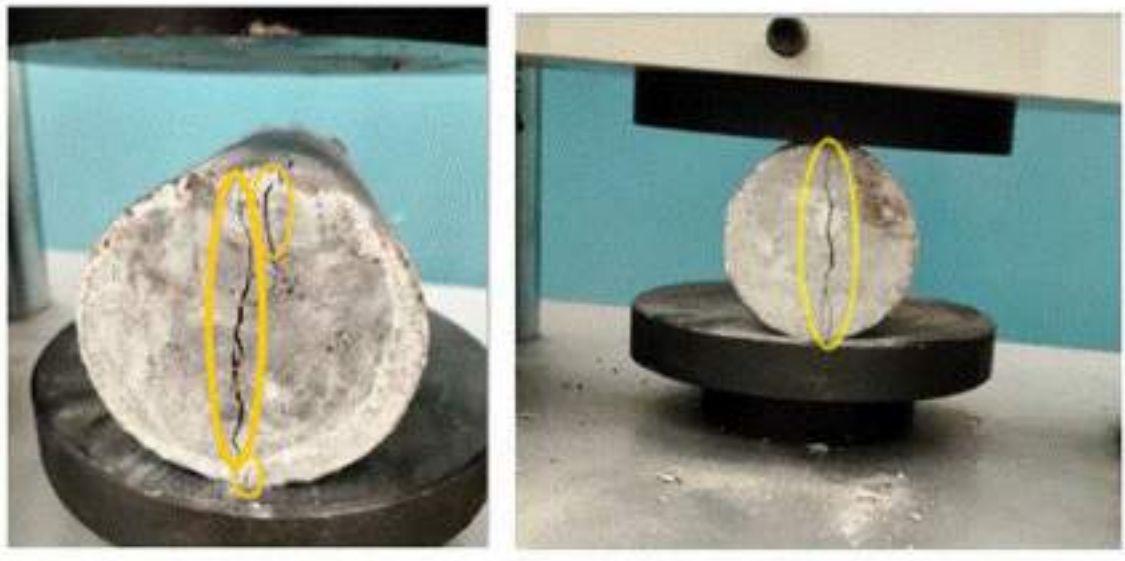

Fig 13. Failure patterns of UHPGPC under tensile load; (a) M1-GW-15, (b) M3-WRP-15.

https://doi.org/10.1371/journal.pone.0285692.g013

Fig 14. Flexural strength of UHPGPC (MPa).

https://doi.org/10.1371/journal.pone.0285692.g014

mixture at 28 and 90 days, the flexural strength of UHPGPC with marble waste reduced by 26.12%, 22.42% (at 5% MW), 28.61%, 24.32%, (at 10% MW), and 31.25%, 27.56%, (at 15% MW), respectively. With the addition of WRP from 5% to 15%, the flexural strength of UHPGPC was reduced by 29.4%, 27.3% (at 5% WRP), 32.1%, 30.2% (at 10% WRP), and 35.3%, 33.7% (at 15% WRP), respectively. The improvement in the flexural strength due to the addition of glass waste could be attributed to the excellent bonding of glass materials and geopolymer gel and the good performance of glass material due to its inherent characteristics, which further reinforced the concrete's matrix, resulting in a dense concrete [36, 86]. From Fig 15A and 15B, it can be observed that the concrete beam with 15% glass waste had better performance as it was cracked in only one place, which signifies the excellent mutual performance of steel fibers and the glass waste in the geopolymer concrete's matrix, whereas, the sample with 15% WRP showed that while loading the concrete sample failed suddenly in two pieces giving no warning of being failed.

5.3 Durability characteristics

5.3.1 Rapid Chloride Penetration test (RCPT). During RCPT, it is presumed that the flow travels over the concrete's specimen by the pore solution, which behaves as an electrolyte. As the proportion and continuousness of pores in the specimens impact the channel of ions and hence impact the rate of flowing current, porous specimens with continued pores probably have higher flow passing, and less porous specimens have lower flow passing. In ultra-high-performance concrete, the water-to-binder ratio has resulted in the development of packed micro-structure in the concrete's matrix, significantly decreasing permeability. Per

Fig 15. Failure patterns of UHPGPC under flexural load; (a) M1-GW-15, (b) M3-WRP-15.

https://doi.org/10.1371/journal.pone.0285692.g015

Table 4, including steel fibers has reduced the current rate and improved the concrete's durability by restricting crack formation due to the plastic and drying shrinkage, leading to reduced permeability [87]. Ghahari et al. [88] performed the SEM analysis of fiber-reinforced concrete. They revealed that adding fibers and developing calcium-silicate-hydrate and bonding among them decreases the concrete's conductivity, which augments the concrete resistance against infiltration of chloride ions. Abbas et al. [87] performed a MIP test, revealing that introducing steel fibers reduced the permeability and augmented the durability.

Table 4. Values of rapid chloride penetration test.

Mix ID	Q (Coulombs)	RCPT Value
Control	1357	Low
M1-GW-5	1341	Low
M1-GW-10	1219	Low
M1-GW-15	964	Very Low
M2-MW-5	1742	Low
M2-MW-10	1421	Low
M2-MW-10	1368	Low
M3- WRP -5	2003	Moderate
M3- WRP -10	2142	Moderate
M3-WRP-15	2264	Moderate

https://doi.org/10.1371/journal.pone.0285692.t004

Furthermore, a packed matrix between geopolymer gel and steel fibers was observed, in among all of the mixtures, M1-GW-15 had the lowermost RCPT value, which signifies reduced permeability due to the very low porosity. The highest values of RCPT were observed in M3-WRP-15, which showed moderate permeability owing to high porosity. All the values of RCPT are presented in Table 4, and the values of RCPT are observed as per the standard values of RCPT shown in Table 5.

5.3.2 Electrical Resistivity (ER). The concrete's ER is a technique to evaluate the concrete's behavior related to penetrating chloride ions. In porous concrete, the ER is low; hence, the infiltration of chloride ions is high. Contrasting to RCPT, ER doesn't heat the concrete specimen, and this test gets completed within a minute, which makes this test very quick. The outcome of electrical resistivity is presented in Table 6. During this test, a reduction in ER signifies decreased proportion behavior. To apply a similar method compared to the results of various tests carried out on durability, comparing the behavior of mixtures based on the specific electrical conductivity index, which is the opposite/inverse of the ER, has also been performed. In M3-WRP-15, high ion concentrations were passed, which makes it highly porous. Adam et al. [89] evaluated the penetration of chloride ions in geopolymer concrete. They revealed the existence of free ions due to the high concentration of alkali chemicals. They reported that by decreasing the NaOH proportion, which means a reduction in the concentration of ions in the pore solution, the conductivity proportion reduces, and thus, the flow proportion reduces. Due to multiple factors, adding steel fibers in UHPGC can lower the flow of charge during electrical resistivity and rapid chloride penetration tests. Primarily, steel fibers can enhance the microstructure of UHPGC, resulting in a denser and more refined pore structure, which impedes the flow of electrical current and the penetration of chloride ions. The steel fibers also help bridge microcracks, which can contribute to reduced electrical conductivity and chloride ion ingress [51, 90, 91]. The presence of steel fibers may also cause a tortuous path for ions to travel through the concrete, leading to higher electrical resistance. These

Table 5. Penetration of chloride ions based on the passing of charges.

Passing of Charge (Coulombs)	RCPT Value
Less than 100	Negligible
100 to 1000	Very low
1000 to 2000	Low
2000 to 4000	Moderate
More than 4000	High

https://doi.org/10.1371/journal.pone.0285692.t005

Table 6. Outcome of electrical resistivity of GPC.

Mix ID	Values of ER (Ω.m)	Specific Electrical Conductivity Index (Ω.m)	Possibility of corrosion
Control	2806	0.000356	Not Likely
M1-GW-5	2793	0.000358	Not Likely
M1-GW-10	2717	0.000368	Not Likely
M1-GW-15	2646	0.000377	Not Likely
M2-MW-5	2901	0.000344	Not Likely
M2-MW-10	2894	0.000345	Not Likely
M2-MW-10	2846	0.000351	Not Likely
M3- WRP -5	2963	0.000337	Not Likely
M3- WRP -10	3014	0.000331	Not Likely
M3-WRP-15	3201	0.000312	Not Likely

https://doi.org/10.1371/journal.pone.0285692.t006

factors, combined, result in lower charge flow and increased resistance to chloride penetration in UHPGC-containing steel fibers. In past research [58–60], GPC depicts a high current flow rate compared to conventional concrete, which isn't due to the lower resistivity against chloride ions. Still, it is also due to the concentration of ions in the concrete's pore solution and the micro-structure of GPC.

5.4 Microstructural analysis

5.4.1 Mercury Intrusion Porosimetry (MIP) analysis. Fig 16 presents mercury intrusion porosimetry of the cumulative porosity of the UHPGPC's specimens. The pore structure of concrete specimens conforms with the findings of past research. M1-GW-15 had a reduced porosity compared to M2-MW-15 and M3-WRP-15, which translates well with the result tendencies in the compression strength. The effect of small particle sizes of glass waste (GW) and marble waste (MW) on porosity and pore connectivity in ultra-high-performance geopolymer concrete (UHPGC) can be considered by examining the microstructure, packing density, and particle size distribution of these materials. Fine particles can fill the voids between larger particles, leading to a denser microstructure and reduced porosity. Selecting a suitable combination of particle sizes for GW and MW is essential to optimize the packing density. Furthermore, the pozzolanic reactivity of these materials plays a crucial role in pore refinement. As glass waste and marble waste react with the alkaline activators in the geopolymer matrix, they form additional geopolymer products, which can fill the pores and improve the overall performance of the UHPGC [92]. The concrete comprising waste rubber powder had the maximum total pore volume, which implies that the mixture has the maximum pore structure and reduced effectiveness in the reaction of the geo-polymerization. Compared with the reference mixture at a pore diameter of 0.031 microns, the cumulative porosity was considerably raised by 29.53%, 43.78%, and 55.61% at 15% substitution of sand with GW, MW and WRP, respectively. From the x-ray diffraction spectra, employing the GW develops extra phases over the curing method. This phase resulted in low porosity and packed microstructure. Lastly, a change in pore size distribution is associated with a variation in the concrete's microstructure, which clarifies some of the strength characteristics [93, 94].

5.4.2 Thermogravimetric analysis (TGA). Fig 17A presents the TGA curve of UHPGPC at 90 days. The phases of loss in mass developed by the dehydration of calcium-aluminate-silicate-hydrate for the UHPGPC; also, due to the accessibility of hydroxyl ions (OH^-), a strong peak related to the calcite phase is noticeable in every mix. Moreover, the weight loss of the UHPGPC is classified into 4 levels. The 1st and 2nd levels corresponded to significant mass loss under 250˚C. The 1st level (approx. 50˚C to 160˚C) is related to the vanishing of available

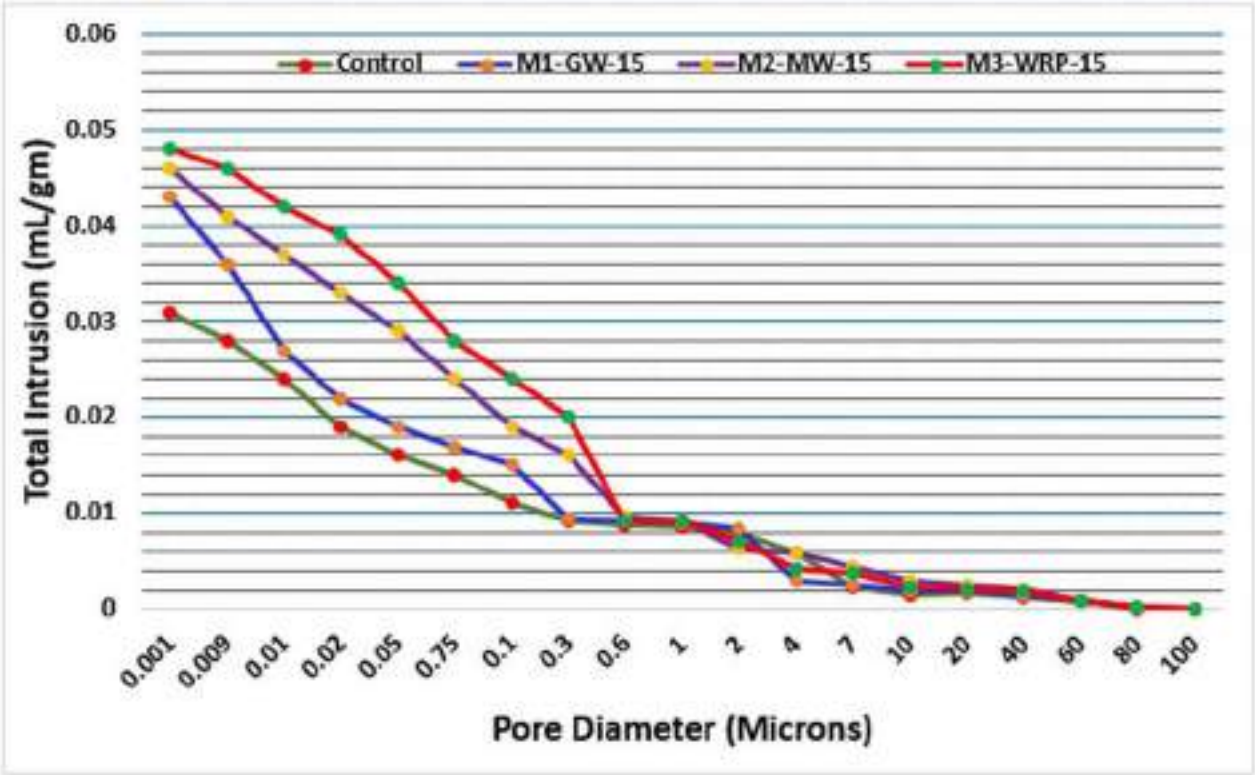

Fig 16. Total porosity of UHPGPC by MIP test at 90 days.

https://doi.org/10.1371/journal.pone.0285692.g016

water, while the 2nd level (approx. 160˚C to 250˚C) concerns confined-water vanishing. The vanishing of physically-chemically restricted water and the hydroxyl poly-condensation method (OH^-) of geopolymer gel are ascribed to the 3rd level (approx. 250˚C to 750˚C). At elevated heating conditions, the 4th level (approx. 750˚C to 1100˚C) is related to the severance of inorganic carbonate compounds (see Fig 17B). It could be observed that the reference mixture loses nearly 6.24%, whereas the UHPGPC comprising 15 glass waste loses 7.19%. The TGA curves in 1st and 2nd phases showed a 5.43%, 6.07%, and 5.65% loss in weight of M1-GW-15, M2-MW-15, and M3-WRP-15, respectively, from the ambient surroundings to 250˚C, whereas the reference mixture at the similar heating condition lost 4.26%.

The improved TGA results by GW can be attributed to the pozzolanic activity and the inherent thermal stability of the glass waste particles. When glass waste reacts with the alkaline activators in the geopolymer matrix, it forms a more stable and thermally resistant structure due to the additional geopolymer products generated through the reaction [95]. The 15% glass waste replacement demonstrated superior thermogravimetric behavior compared to all other modified mixtures. This outcome suggests that the higher glass waste content optimizes the balance between particle packing and pozzolanic activity. This leads to a more thermally stable geopolymer matrix that resists degradation and weight loss under high temperatures. The presence of double-hooked end steel fibers in UHPGPC could also play a role in enhancing the material's thermogravimetric behavior. These steel fibers can create a reinforcing network throughout the geopolymer matrix, providing improved load transfer and potentially enhancing the overall thermal stability of the composite material. The optimal performance observed with the 15% glass waste replacement might be attributed to the combined effect of the improved glass waste microstructure and the steel fibers' reinforcing action. It is essential to consider that marble

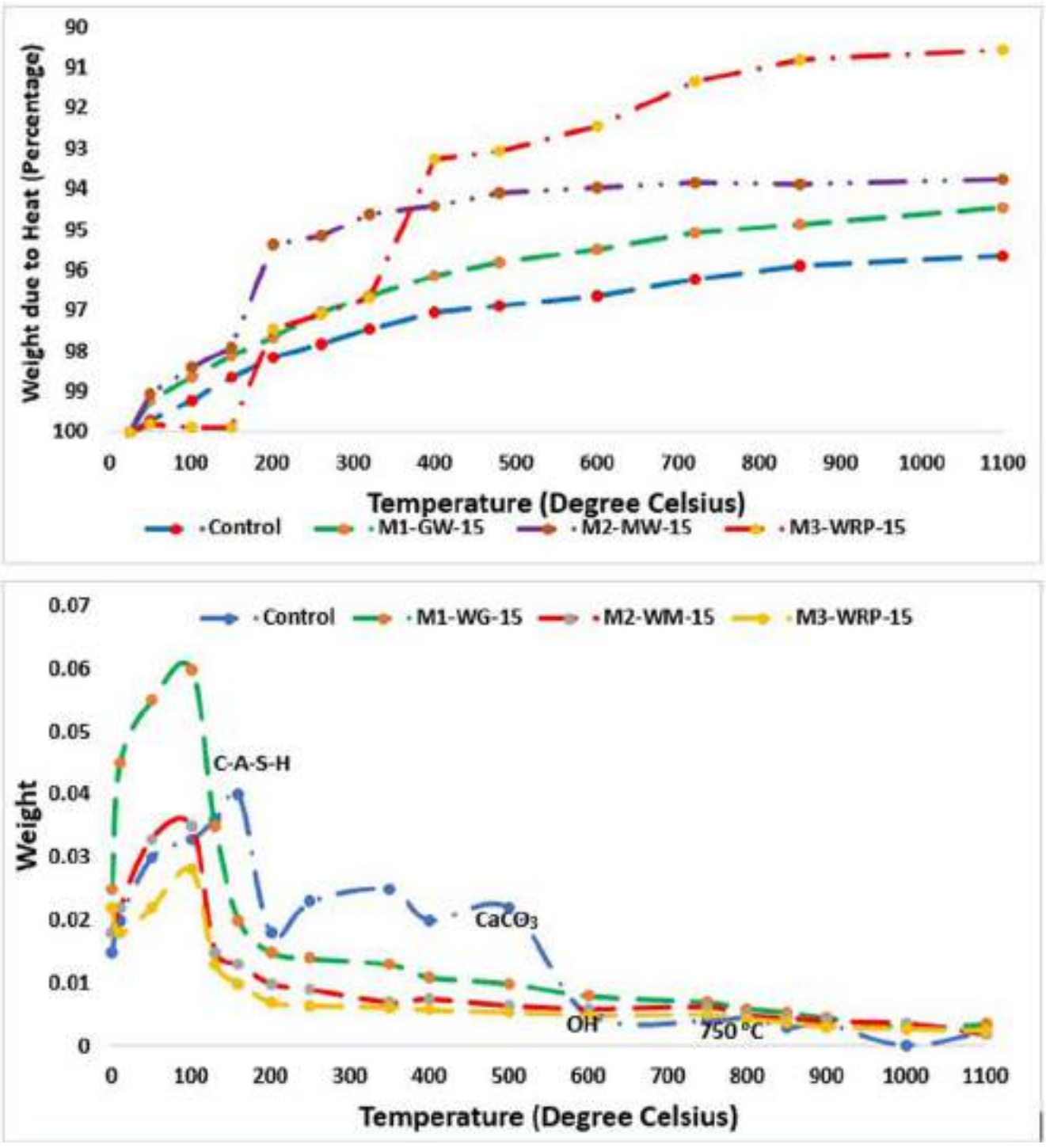

Fig 17. (a) TGA analysis of UHPGPC. (b) Derivative Thermogravimetric Curve of UHPGPC.

https://doi.org/10.1371/journal.pone.0285692.g017

waste and waste rubber powder have different thermal properties compared to glass waste, which could affect the thermogravimetric behavior of the UHPGPC [96, 97]. These materials

might not contribute to forming a thermally stable geopolymer matrix to the same extent as glass waste, leading to less favorable TGA results.

5.4.3 X-ray diffraction (XRD) analysis. The incorporation of glass waste, marble waste, and waste rubber powder into ultra-high-performance geopolymer concrete (UHPGPC) can significantly influence the X-ray diffraction (XRD) analysis results due to their distinct mineralogical compositions and reactivity. Glass waste, being amorphous and pozzolanic, reacts with the alkaline activators in the geopolymer matrix, leading to the formation of additional geopolymer products, which could be observed as new or enhanced peaks in the XRD pattern [98–100]. Marble waste, primarily composed of calcium carbonate ($CaCO_3$) in calcite, exhibits limited pozzolanic activity. Its addition to UHPGPC might result in the appearance of calcite peaks in the XRD analysis, but it is less likely to contribute to the formation of new geopolymer products. However, marble waste can still affect the geopolymer matrix's particle packing and microstructure [101, 102]. As an organic material, waste rubber powder has a negligible impact on the XRD analysis of UHPGPC as it does not contribute to forming new geopolymer products.

The x-ray diffraction spectra were done on ultra-high-performance geopolymer concrete at 90 days of curing to determine the phase compositions in UHPGPC by adding WPR, GW, and MW. Fig 18 presents the x-ray diffraction spectra of different mixes of UHPGPC. The presence of significant humps in the range of 22 degrees and 32 degrees verifies the presence of shapeless phases (calcium-aluminate-silicate-hydrate) in the GPC. Hence, the main phase comprises albite, SiO_2, calcium-aluminate-silicate-hydrate, and calcite, whereas lower humps of calcite SiO_2 could also be observed. Including glass waste in the mix led to the control of crystal-shaped humps of SiO_2 and calcite. The remaining low humps were related to cristobalite, $CaSiO_3$, and mullite. The humps dispensed to different phases of calcium, classified as hematite, $CaCO_3$, etc., are recognized in the UHPGPC comprising marble waste. Still, their concentration seemed to reduce with time, which implies the slow change in the phase in the presence of the marble waste, which results in the slow and weak process of geo-polymerization and significant loss in mass, as observed during the TGA test. Moreover, the development of SiO_2 and albite was decreased in the samples comprising 15% waste rubber powder, which resulted in a significant reduction of concrete strength (as presented in the strength characteristics section). In addition to the development of calcium-aluminate-silicate-hydrate and potassium-aluminate-silicate-hydrate, it reduces because of the lowered adhesion between geopolymer gel and rubber material to form a porous matrix in concrete [103–105].

6. Sustainability and environmental performance

The development of ultra-high-performance geopolymer concrete (UHPGPC) using ground granulated blast furnace slag (GBFS) and waste silica ash (WSA) as primary binders, along with the incorporation of glass waste, marble waste, and waste rubber powder as partial substitutes for fine aggregates, demonstrates a commitment to sustainable construction practices and enhanced environmental performance. Utilizing these industrial by-products and waste materials in the production of UHPGPC offers numerous sustainability benefits. First, it reduces the consumption of natural resources, such as limestone and sand, thereby minimizing the environmental impact of their extraction, transportation, and processing. This practice also supports conserving finite natural resources, helping ensure their availability for future generations.

Second, replacing Portland cement, a major contributor to greenhouse gas emissions, with GBFS and WSA as geopolymer binders helps reduce the carbon footprint of concrete production. Geopolymer binders are produced using low-energy, low-emission alkaline activation

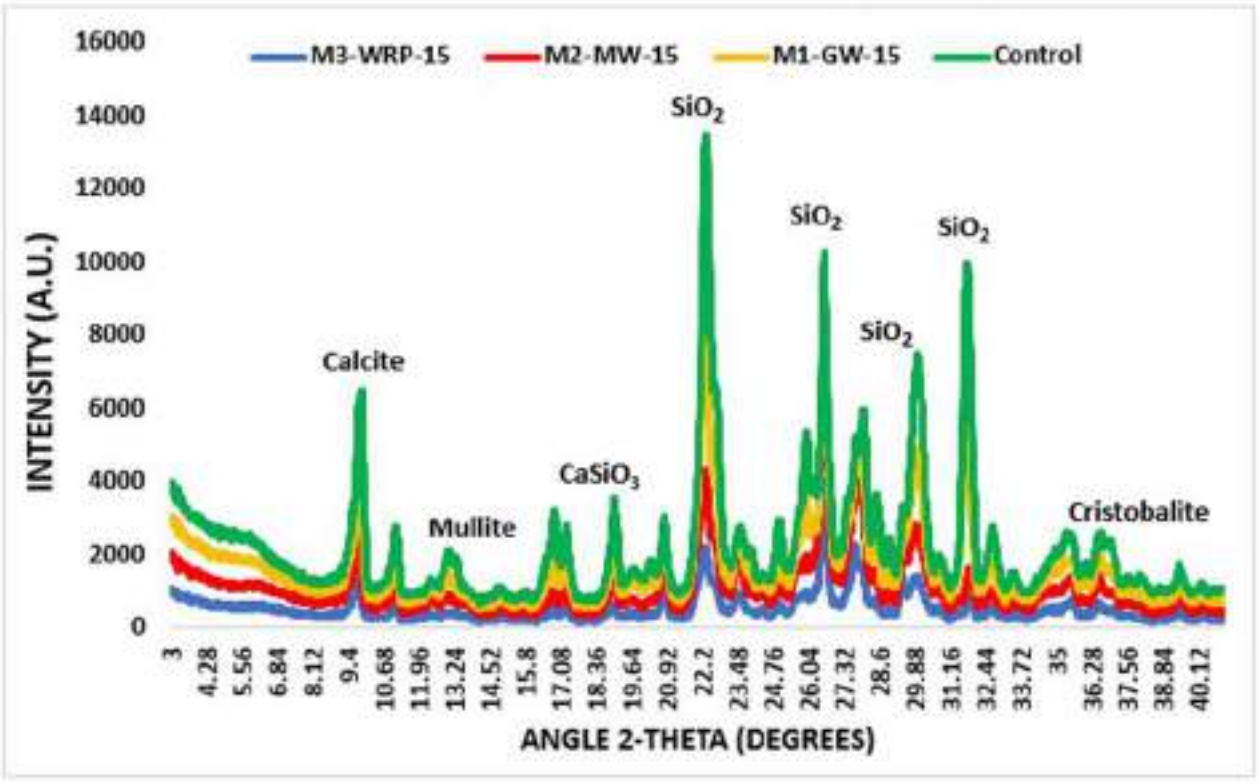

Fig 18. X-ray diffraction analysis of UHPGPC.

https://doi.org/10.1371/journal.pone.0285692.g018

processes, which offer environmental advantages over traditional Portland cement production methods. Incorporating waste materials like glass waste, marble waste, and waste rubber powder as partial substitutes for fine aggregates contributes to effective waste management and promotes a circular economy. By repurposing materials that would otherwise end up in landfills, the environmental impact associated with waste disposal is reduced while conserving natural sand resources. The improved mechanical properties and durability of UHPGPC containing these waste materials result in longer service life and reduced maintenance requirements for the structures built with this concrete. This increased longevity translates to lower life cycle environmental impact and resource consumption associated with construction and infrastructure projects.

Moreover, using UHPGPC with waste materials in construction projects can lead to potential cost savings, as these waste materials are often less expensive than traditional aggregates. This economic advantage encourages adopting sustainable construction practices, further contributing to the broader goals of resource conservation and environmental protection. The present study showed that this innovative approach minimizes the consumption of natural resources, reduces waste generation, and mitigates the environmental impact associated with traditional concrete production, ultimately contributing to a more sustainable future for the construction industry.

7. Conclusions

The fresh, strength and microstructural properties of ultra-high-performance geopolymer concrete comprising waste rubber powder, glass waste, and marble waste as a fractional

replacement of sand at 5%, 10%, and 15% have been investigated. Based on the present research findings, the following conclusions have been attained:

- The addition of glass waste into ultra-high-performance geopolymer concrete augments the fresh properties, whereas the addition of marble waste and waste rubber powder reduces them, specifically at 15% substitution of fine aggregates. The ultra-high-performance geopolymer concrete with the 15% WRP showed a maximum decrease in the slump value by 19.44% compared with the reference mixture.
- Compression, indirect tensile, and flexural strength were improved as the glass waste percentage was raised. Also, in some cases, the strength behavior of concrete with glass waste was similar to the reference mixture due to low porosity and the high proportion of hydration products (calcium-aluminate-silicate-hydrate). The ultra-high-performance geopolymer concrete with glass waste had improved strength behavior compared to marble waste and waste rubber powder.
- In the ER and RCPT tests, introducing steel fibers lowers the flow of charges over the UHPGPC, while concrete with waste rubber powder showed higher porosity with high values of ER and RCPT.
- X-ray diffraction analysis showed that the ultra-high-performance geopolymer concrete with the 15% glass waste had good adhesion among glass particles and gel of geo-polymerization, which is mainly the reason for improvements in the strength attributes of ultra-high-performance geopolymer concrete than the UHPGPC with other discarded materials.
- From the mercury intrusion porosimetry analysis, the addition of waste rubber powder significantly increases the pore diameters and porosity, which can be ascribed to the porous microstructure, which is the reason behind the strength decrease than the reference mixture.
- The percentage of the WRP had a detrimental effect on the thermal response of the specimens as assessed by the TGA test. The reference sample could sustain 93.75% of its weight, whereas adding 15% GW, 15% MW, and 15% WRP led to the loss in concrete weight by 5.64%, 6.25%, and 9.44%, respectively.

Supporting information

S1 File. Contains all the supporting tables.
(XLSX)

Author Contributions

Conceptualization: Fadi Althoey.

Data curation: Saleh Alsulamy.

Methodology: Jesús de Prado Gil.

Resources: Rebeca Martínez-García.

Software: Mohamed M. Arbili.

Validation: Osama Zaid.

Visualization: Osama Zaid.

Writing – original draft: Osama Zaid.

References

1. Guo P, Meng W, Nassif H, et al (2020) New perspectives on recycling waste glass in manufacturing concrete for sustainable civil infrastructure. Constr Build Mater 257:119579. https://doi.org/10.1016/j.conbuildmat.2020.119579
2. Martínez-García R, Jagadesh P, Zaid O, et al (2022) The Present State of the Use of Waste Wood Ash as an Eco-Efficient Construction Material: A Review. Materials (Basel) 15:. https://doi.org/10.3390/ma15155349
3. Worrell E, Price L, Martin N, et al (2001) Carbon Dioxide Emission from the Global Cement Industry. Annu Rev Energy Env 26:303–329. https://doi.org/10.1146/annurev.energy.26.1.303
4. Shahmansouri AA, Akbarzadeh Bengar H, Ghanbari S (2020) Compressive strength prediction of eco-efficient GGBS-based geopolymer concrete using GEP method. J Build Eng 31:101326. https://doi.org/10.1016/j.jobe.2020.101326
5. Imtiaz L, Rehman S, Memon S, et al (2020) A Review of Recent Developments and Advances in Eco-Friendly Geopolymer Concrete. Appl Sci 10:7838. https://doi.org/10.3390/app10217838
6. Qaidi S, Isleem H, Azevedo A, Ahmed H (2022) Sustainable utilization of red mud waste (bauxite residue) and slag for the production of geopolymer composites: A review. Case Stud Constr Mater. https://doi.org/10.1016/j.cscm.2022.e00994
7. Kathirvel P, Sreekumaran S (2021) Sustainable development of ultra high performance concrete using geopolymer technology. J Build Eng 39:102267. https://doi.org/10.1016/j.jobe.2021.102267
8. Luhar S, Cheng T-W, Nicolaides D, et al (2019) Valorisation of glass wastes for the development of geopolymer composites–Durability, thermal and microstructural properties: A review. Constr Build Mater 222:673–687. https://doi.org/10.1016/j.conbuildmat.2019.06.169
9. Khater HM, El-Nagar AM (2020) Preparation of sustainable of eco-friendly MWCNT-geopolymer composites with superior sulfate resistance. Adv Compos Hybrid Mater 3:375–389. https://doi.org/10.1007/s42114-020-00170-4
10. Qaidi SMA, Mohammed AS, Ahmed HU, et al (2022) Rubberized geopolymer composites: A comprehensive review. Ceram Int. https://doi.org/10.1016/j.ceramint.2022.06.123
11. He X, Yuhua Z, Qaidi S, et al (2022) Mine tailings-based geopolymers: A comprehensive review. Ceram Int. https://doi.org/10.1016/j.ceramint.2022.05.345
12. Zaid O, Martínez-García R, Abadel AA, et al (2022) To determine the performance of metakaolin-based fiber-reinforced geopolymer concrete with recycled aggregates. Arch Civ Mech Eng 22:114. https://doi.org/10.1007/s43452-022-00436-2
13. Smirnova O, Menéndez-Pidal I, Alekseev A, et al (2022) Strain Hardening of Polypropylene Microfiber Reinforced Composite Based on Alkali-Activated Slag Matrix. Materials (Basel) 15:1607. https://doi.org/10.3390/ma15041607 PMID: 35208146
14. Smirnova O, Kazanskaya L, Koplík J, et al (2021) Concrete Based on Clinker-Free Cement: Selecting the Functional Unit for Environmental Assessment. Sustainability 13:. https://doi.org/10.3390/su13010135
15. SO M. (2020) Low-Clinker Cements with Low Water Demand. J Mater Civ Eng 32:6020008. https://doi.org/10.1061/(ASCE)MT.1943-5533.0003241
16. Qian D, Yu R, Shui Z, et al (2020) A novel development of green ultra-high performance concrete (UHPC) based on appropriate application of recycled cementitious material
17. Liu Y, Shi C, Zhang Z, et al (2020) Mechanical and fracture properties of ultra-high performance geopolymer concrete: Effects of steel fiber and silica fume. Cem Concr Compos 112:103665. https://doi.org/10.1016/j.cemconcomp.2020.103665
18. Rossi L, Lima L, Sun Y, et al (2023) Future perspectives for alkali-activated materials: from existing standards to structural applications. RILEM Tech Lett 7:159–177. https://doi.org/10.21809/rilemtechlett.2022.160
19. Palomo A, Maltseva O, García-Lodeiro I, Fernández-Jiménez A (2021) Portland Versus Alkaline Cement: Continuity or Clean Break: "A Key Decision for Global Sustainability". Front Chem 9:705475. https://doi.org/10.3389/fchem.2021.705475 PMID: 34712645
20. Pyo S, Kim H-K (2017) Fresh and hardened properties of ultra-high performance concrete incorporating coal bottom ash and slag powder. Constr Build Mater 131:459–466. https://doi.org/10.1016/j.conbuildmat.2016.10.109
21. Liew KM, Sojobi AO, Zhang LW (2017) Green concrete: Prospects and challenges. Constr Build Mater 156:1063–1095. https://doi.org/10.1016/j.conbuildmat.2017.09.008

22. Yakovlev G, Пок И, Gordina A, et al (2021) Influence of Sulphate Attack on Properties of Modified Cement Composites. Appl Sci 11:8509. https://doi.org/10.3390/app11188509
23. Smirnova O (2019) Compatibility of shungisite microfillers with polycarboxylate admixtures in cement compositions. ARPN J Eng Appl Sci 14:600–610.
24. Smirnova O (2018) Development of classification of rheologically active microfillers for disperse systems with Portland cement and superplasticizer. Int J Civ Eng Technol 9:1966–1973.
25. Smirnova O (2018) Technology of increase of nanoscale pores volume in protective cement matrix. Int J Civ Eng Technol 9:1991–2000.
26. Wu Z, Shi C, He W (2017) Comparative study on flexural properties of ultra-high performance concrete with supplementary cementitious materials under different curing regimes. Constr Build Mater 136:307–313. https://doi.org/10.1016/j.conbuildmat.2017.01.052
27. Provis J, Van Deventer J (2009) Geopolymers: Structures, processing, properties and industrial applications.
28. Yu R, Spiesz P, Brouwers HJH (2015) Development of an eco-friendly Ultra-High Performance Concrete (UHPC) with efficient cement and mineral admixtures uses. Cem Concr Compos 55:383–394. https://doi.org/10.1016/j.cemconcomp.2014.09.024
29. Saidova Z, Yakovlev G, Smirnova O, et al (2021) Modification of Cement Matrix with Complex Additive Based on Chrysotyl Nanofibers and Carbon Black. Appl Sci 11:6943. https://doi.org/10.3390/app11156943
30. Amin M, Tayeh BA, Agwa IS (2020) Effect of using mineral admixtures and ceramic wastes as coarse aggregates on properties of ultrahigh-performance concrete. J Clean Prod 273:123073. https://doi.org/10.1016/j.jclepro.2020.123073
31. Romagnoli M (2015) Handbook of Alkali-Activated Cements, Mortars and Concretes. or 133–170.
32. He P, Wang M, Fu S, et al (2016) Effects of Si/Al ratio on the structure and properties of metakaolin based geopolymer. Ceram Int 42:14416–14422. https://doi.org/10.1016/j.ceramint.2016.06.033
33. Pacheco-Torgal F, Chindaprasirt P, Ozbakkaloglu T (2022) 1—Introduction. In: Pacheco-Torgal F, Chindaprasirt P, Ozbakkaloglu T (arg) Handbook of Advances in Alkali-Activated Concrete. Woodhead Publishing, or 1–12.
34. Taher SMS, Saadullah ST, Haido JH, Tayeh BA (2021) Behavior of geopolymer concrete deep beams containing waste aggregate of glass and limestone as a partial replacement of natural sand. Case Stud Constr Mater 15:e00744. https://doi.org/10.1016/j.cscm.2021.e00744
35. Shoaei P, Musaeei HR, Mirlohi F, et al (2019) Waste ceramic powder-based geopolymer mortars: Effect of curing temperature and alkaline solution-to-binder ratio. Constr Build Mater 227:116686. https://doi.org/10.1016/j.conbuildmat.2019.116686
36. Youssf O, Elchalakani M, Hassanli R, et al (2022) Mechanical performance and durability of geopolymer lightweight rubber concrete. J Build Eng 45:103608. https://doi.org/10.1016/j.jobe.2021.103608
37. Smirnova OM, de Navascués I, Mikhailevskii VR, et al (2021) Sound-Absorbing Composites with Rubber Crumb from Used Tires. Appl Sci 11:. https://doi.org/10.3390/app11167347
38. Mermerdaş K, Arbili MM (2015) Explicit formulation of drying and autogenous shrinkage of concretes with binary and ternary blends of silica fume and fly ash. Constr Build Mater 94:371–379. https://doi.org/10.1016/j.conbuildmat.2015.07.074
39. Ambily PS, Ravisankar K, Umarani C, et al (2014) Development of ultra-high-performance geopolymer concrete. Mag Concr Res 66:82–89. https://doi.org/10.1680/macr.13.00057
40. Wetzel A, Middendorf B (2019) Influence of silica fume on properties of fresh and hardened ultra-high performance concrete based on alkali-activated slag. Cem Concr Compos 100:53–59. https://doi.org/10.1016/j.cemconcomp.2019.03.023
41. Althoey F, Zaid O, Alsulamy S, et al (2023) Experimental study on the properties of ultra-high-strength geopolymer concrete with polypropylene fibers and nano-silica. PLoS One 18:1–31. https://doi.org/10.1371/journal.pone.0282435
42. Zaid O, Mukhtar FM, M-García R, et al (2022) Characteristics of high-performance steel fiber reinforced recycled aggregate concrete utilizing mineral filler. Case Stud Constr Mater 16:e00939. https://doi.org/10.1016/j.cscm.2022.e00939
43. Aslam F, Zaid O, Althoey F, et al Evaluating the influence of fly ash and waste glass on the characteristics of coconut fibers reinforced concrete. Struct Concr n/a: https://doi.org/10.1002/suco.202200183
44. Zaid O, Ahmad J, Siddique MS, et al (2021) A step towards sustainable glass fiber reinforced concrete utilizing silica fume and waste coconut shell aggregate. Sci Rep 11:1–14.

45. Zaid O, Ahmad J, Siddique MS, Aslam F (2021) Effect of Incorporation of Rice Husk Ash Instead of Cement on the Performance of Steel Fibers Reinforced Concrete. Front Mater 8:14–28. https://doi.org/10.3389/fmats.2021.665625

46. Althoey F, Zaid O, Alsharari F, et al (2022) Evaluating the impact of nano-silica on characteristics of self-compacting geopolymer concrete with waste tire steel fiber. Arch Civ Mech Eng 23:48. https://doi.org/10.1007/s43452-022-00587-2

47. Althoey F, Zaid O, Martínez-García R, et al (2023) Impact of Nano-silica on the hydration, strength, durability, and microstructural properties of concrete: A state-of-the-art review. Case Stud Constr Mater 18:e01997. https://doi.org/10.1016/j.cscm.2023.e01997

48. Althoey F, Zaid O, Arbili MM, et al (2023) Physical, strength, durability and microstructural analysis of self-healing concrete: A systematic review. Case Stud Constr Mater 18:e01730. https://doi.org/10.1016/j.cscm.2022.e01730

49. Osama Zaid; Rebeca Martínez-García; Fahid Aslam (2022) Influence of Wheat Straw Ash as Partial Substitute of Cement on Properties of High-Strength Concrete Incorporating Graphene Oxide. J Mater Civ Eng. https://doi.org/10.1061/(ASCE)MT.1943-5533.0004415

50. Sabireen, Butt F, Ahmad A, et al (2023) Mechanical performance of fiber-reinforced concrete and functionally graded concrete with natural and recycled aggregates. Ain Shams Eng J 102121. https://doi.org/10.1016/j.asej.2023.102121

51. Mousavinejad SHG, Sammak M (2021) Strength and chloride ion penetration resistance of ultra-high-performance fiber reinforced geopolymer concrete. Structures 32:1420–1427. https://doi.org/10.1016/j.istruc.2021.03.112

52. Ahmad J, Aslam F, Zaid O, et al (2021) Self-Fibers Compacting Concrete Properties Reinforced with Propylene Fibers. Sci Eng Compos Mater 28:64–72.

53. Althoey F, Zaid O, de-Prado-Gil J, et al (2022) Impact of sulfate activation of rice husk ash on the performance of high strength steel fiber reinforced recycled aggregate concrete. J Build Eng 54:104610. https://doi.org/10.1016/j.jobe.2022.104610

54. Zaid O, Hashmi SRZ, Aslam F, et al (2022) Experimental study on the properties improvement of hybrid graphene oxide fiber-reinforced composite concrete. Diam Relat Mater 108883. https://doi.org/10.1016/j.diamond.2022.108883

55. Maglad AM, Zaid O, Arbili MM, et al (2022) A Study on the Properties of Geopolymer Concrete Modified with Nano Graphene Oxide. Buildings 12:. https://doi.org/10.3390/buildings12081066

56. Ahmad J, Zaid O, Pérez CL-C, et al (2022) Experimental Research on Mechanical and Permeability Properties of Nylon Fiber Reinforced Recycled Aggregate Concrete with Mineral Admixture. Appl Sci 12:. https://doi.org/10.3390/app12020554

57. Ahmad J, Zaid O, Aslam F, et al (2021) A Study on the Mechanical Characteristics of Glass and Nylon Fiber Reinforced Peach Shell Lightweight Concrete. Materials (Basel) 14:21–41. https://doi.org/10.3390/ma14164488

58. Liu Y, Zhang Z, Shi C, et al (2020) Development of ultra-high performance geopolymer concrete (UHPGC): Influence of steel fiber on mechanical properties. Cem Concr Compos 112:103670. https://doi.org/10.1016/j.cemconcomp.2020.103670

59. Amin M, Zeyad AM, Tayeh BA, Saad Agwa I (2022) Effect of ferrosilicon and silica fume on mechanical, durability, and microstructure characteristics of ultra high-performance concrete. Constr Build Mater 320:126233. https://doi.org/10.1016/j.conbuildmat.2021.126233

60. ASTM C 1437 Standard Test Method For Flow Of Hydraulic Cement Mortar.

61. International A (2019) Time of Setting of Hydraulic Cement by Vicat Needle ASTM C-191-19. Annu B ASTM Stand 191–19 1–10.

62. ASTM C 39 (2017) Standard test method for compressive strength of cylindrical concrete specimens. Am Soc Test Mater ASTM, West Conshohocken.

63. ASTM C 496/-11 (2011) Standard Test Method for Splitting Tensile Strength of Cylindrical Concrete Specimens.

64. ASTM C469 Standard Test Method for Static Modulus of Elasticity and Poisson's Ratio of Concrete in Compression.

65. ASTM C (2010) Standard test method for flexural strength of concrete (using simple beam with third-point loading). In: American Society for Testing and Materials. or 12959–19428.

66. ASTM C 1202 (2009) Standard test method for electrical induction of concrete, stability to resist chloride ion penetration. American Society for Testing and Materials International, West Conshohocken.

67. Luhar S, Cheng T-W, Nicolaides D, et al (2019) Valorisation of glass waste for development of Geopolymer composites–Mechanical properties and rheological characteristics: A review. Constr Build Mater 220:547–564. https://doi.org/10.1016/j.conbuildmat.2019.06.041

68. Atyia MM, Mahdy MG, Abd Elrahman M (2021) Production and properties of lightweight concrete incorporating recycled waste crushed clay bricks. Constr Build Mater 304:124655. https://doi.org/10.1016/j.conbuildmat.2021.124655

69. Omer SA, Demirboga R, Khushefati WH (2015) Relationship between compressive strength and UPV of GGBFS based geopolymer mortars exposed to elevated temperatures. Constr Build Mater 94:189–195. https://doi.org/10.1016/j.conbuildmat.2015.07.006

70. El-Sayed TA (2021) Axial Compression Behavior of Ferrocement Geopolymer HSC Columns. Polymers (Basel) 13:. https://doi.org/10.3390/polym13213789 PMID: 34771346

71. Salih APDM, Ali A, Farzadnia N (2014) Characterization of mechanical and microstructural properties of palm oil fuel ash geopolymer cement paste. Constr Build Mater 65:592–603. https://doi.org/10.1016/j.conbuildmat.2014.05.031

72. Turner LK, Collins FG (2013) Carbon dioxide equivalent (CO2-e) emissions: A comparison between geopolymer and OPC cement concrete. Constr Build Mater 43:125–130. https://doi.org/10.1016/j.conbuildmat.2013.01.023

73. Ding M, Yu R, Feng Y, et al (2021) Possibility and advantages of producing an ultra-high performance concrete (UHPC) with ultra-low cement content. Constr Build Mater 273:122023. https://doi.org/10.1016/j.conbuildmat.2020.122023

74. Tahwia AM, Elgendy GM, Amin M (2021) Durability and microstructure of eco-efficient ultra-high-performance concrete. Constr Build Mater 303:124491. https://doi.org/10.1016/j.conbuildmat.2021.124491

75. John SK, Nadir Y, Girija K (2021) Effect of source materials, additives on the mechanical properties and durability of fly ash and fly ash-slag geopolymer mortar: A review. Constr Build Mater 280:122443. https://doi.org/10.1016/j.conbuildmat.2021.122443

76. Dakhane A, Tweedley S, Kailas S, et al (2017) Mechanical and microstructural characterization of alkali sulfate activated high volume fly ash binders. Mater Des 122:236–246. https://doi.org/10.1016/j.matdes.2017.03.021

77. Tayeh BA, Akeed MH, Qaidi S, Bakar BHA (2022) Influence of microsilica and polypropylene fibers on the fresh and mechanical properties of ultra-high performance geopolymer concrete (UHP-GPC). Case Stud Constr Mater 17:e01367. https://doi.org/10.1016/j.cscm.2022.e01367

78. Albitar M, Visintin P, Mohamed Ali MS, Drechsler M (2015) Assessing behaviour of fresh and hardened geopolymer concrete mixed with class-F fly ash. KSCE J Civ Eng 19:1445–1455. https://doi.org/10.1007/s12205-014-1254-z

79. Nath P, Sarker P (2017) Flexural strength and elastic modulus of ambient-cured blended low-calcium fly ash geopolymer concrete. Constr Build Mater 130:22–31. https://doi.org/10.1016/j.conbuildmat.2016.11.034

80. Zhang P, Wang K, Wang J, et al (2020) Mechanical properties and prediction of fracture parameters of geopolymer/alkali-activated mortar modified with PVA fiber and nano-SiO2. Ceram Int 46:20027–20037. https://doi.org/10.1016/j.ceramint.2020.05.074

81. Lee W-H, Wang J-H, Ding Y-C, Cheng T-W (2019) A study on the characteristics and microstructures of GGBS/FA based geopolymer paste and concrete. Constr Build Mater 211:807–813. https://doi.org/10.1016/j.conbuildmat.2019.03.291

82. Ekinci E, Türkmen İ, Kantarci F, Karakoç MB (2019) The improvement of mechanical, physical and durability characteristics of volcanic tuff based geopolymer concrete by using nano silica, micro silica and Styrene-Butadiene Latex additives at different ratios. Constr Build Mater 201:257–267. https://doi.org/10.1016/j.conbuildmat.2018.12.204

83. Khan I, Abegaz G, Jaleta B (2021) A high-performance geopolymer concrete an experimental study using fly ash, GGBS and copper slag. J Struct Eng 48:71–84.

84. Tay P, Mazlan N (2021) Mechanical Strength of Graphene Reinforced Geopolymer Nanocomposites: A Review. Front Mater 8:661013. https://doi.org/10.3389/fmats.2021.661013

85. Jain A, Gupta R, Chaudhary S (2019) Performance of self-compacting concrete comprising granite cutting waste as fine aggregate. Constr Build Mater 221:539–552. https://doi.org/10.1016/j.conbuildmat.2019.06.104

86. Angelin Lincy G, Velkennedy R (2021) Experimental optimization of metakaolin and nanosilica composite for geopolymer concrete paver blocks. Struct Concr 22:E442–E451. https://doi.org/10.1002/suco.201900555

87. Abbas S, Soliman AM, Nehdi ML (2015) Exploring mechanical and durability properties of ultra-high performance concrete incorporating various steel fiber lengths and dosages. Constr Build Mater 75:429–441. https://doi.org/10.1016/j.conbuildmat.2014.11.017

88. Ramezanianpour AA, Esmaeili M, Ghahari SA, Najafi MH (2013) Laboratory study on the effect of polypropylene fiber on durability, and physical and mechanical characteristic of concrete for application in sleepers. Constr Build Mater 44:411–418. https://doi.org/10.1016/j.conbuildmat.2013.02.076

89. Adam A (2009) Strength and durability properties of alkali activated slag and fly ash-based geopolymer concrete.

90. Gunasekara C, Law D, Bhuiyan S, et al (2019) Chloride induced corrosion in different fly ash based geopolymer concretes. Constr Build Mater 200:502–513. https://doi.org/10.1016/j.conbuildmat.2018.12.168

91. Noushini A, Castel A, Aldred J, Rawal A (2020) Chloride diffusion resistance and chloride binding capacity of fly ash-based geopolymer concrete. Cem Concr Compos 105:103290. https://doi.org/10.1016/j.cemconcomp.2019.04.006

92. Mu S, Liu J, Lin W, et al (2017) Property and microstructure of aluminosilicate inorganic coating for concrete: Role of water to solid ratio. Constr Build Mater 148:846–856. https://doi.org/10.1016/j.conbuildmat.2017.05.070

93. Cai R, Ye H (2021) Clinkerless ultra-high strength concrete based on alkali-activated slag at high temperatures. Cem Concr Res 145:106465. https://doi.org/10.1016/j.cemconres.2021.106465

94. Duan P, Shui Z, Chen W, Shen C (2013) Effects of metakaolin, silica fume and slag on pore structure, interfacial transition zone and compressive strength of concrete. Constr Build Mater 44:1–6. https://doi.org/10.1016/j.conbuildmat.2013.02.075

95. Luhar S, Chaudhary S, Luhar I (2018) Thermal resistance of fly ash based rubberized geopolymer concrete. J Build Eng 19:420–428. https://doi.org/10.1016/j.jobe.2018.05.025

96. Thirunavukarasu R, Jeyalakshmi R, Parshwanath R (2018) Study on the role of n-SiO2 incorporation in thermo-mechanical and microstructural properties of ambient cured FA-GGBS geopolymer matrix. Appl Surf Sci 449:. https://doi.org/10.1016/j.apsusc.2018.01.281

97. Hussin MW, Bhutta MAR, Azreen M, et al (2015) Performance of blended ash geopolymer concrete at elevated temperatures. Mater Struct 48:709–720. https://doi.org/10.1617/s11527-014-0251-5

98. Zhao R, Yuan Y, Cheng Z, et al (2019) Freeze-thaw resistance of Class F fly ash-based geopolymer concrete. Constr Build Mater 222:474–483. https://doi.org/10.1016/j.conbuildmat.2019.06.166

99. Adak D, Sarkar M, Mandal S (2014) Effect of nano-silica on strength and durability of fly ash based geopolymer mortar. Constr Build Mater 70:453–459. https://doi.org/10.1016/j.conbuildmat.2014.07.093

100. Tuyan M, Andiç-Çakir Ö, Ramyar K (2018) Effect of alkali activator concentration and curing condition on strength and microstructure of waste clay brick powder-based geopolymer. Compos Part B Eng 135:242–252. https://doi.org/10.1016/j.compositesb.2017.10.013

101. Mustakim SM, Das SK, Mishra J, et al (2021) Improvement in Fresh, Mechanical and Microstructural Properties of Fly Ash- Blast Furnace Slag Based Geopolymer Concrete By Addition of Nano and Micro Silica. Silicon 13:2415–2428. https://doi.org/10.1007/s12633-020-00593-0

102. Zawrah MF, Abo Sawan SE, Khattab RM, Abdel-Shafi AA (2020) Effect of nano sand on the properties of metakaolin-based geopolymer: Study on its low rate sintering. Constr Build Mater 246:118486. https://doi.org/10.1016/j.conbuildmat.2020.118486

103. Ariffin MAM, Bhutta MAR, Hussin MW, et al (2013) Sulfuric acid resistance of blended ash geopolymer concrete. Constr Build Mater 43:80–86. https://doi.org/10.1016/j.conbuildmat.2013.01.018

104. Zaharaki D, Galetakis M, Komnitsas K (2016) Valorization of construction and demolition (C&D) and industrial wastes through alkali activation. Constr Build Mater 121:686–693. https://doi.org/10.1016/j.conbuildmat.2016.06.051

105. Ge X, Hu X, Shi C (2022) The effect of different types of class F fly ashes on the mechanical properties of geopolymers cured at ambient environment. Cem Concr Compos 130:104528. https://doi.org/10.1016/j.cemconcomp.2022.104528